AD-A165 229

(12)

AFGL-TR-84-0056

A STUDY OF ATMOSPHERIC REACTIONS OF NEUTRAL SODIUM SPECIES AND OTHER METALS OF METEORIC ORIGIN

J. A. Silver
M. S. Zahniser
C. E. Kolb
A. C. Stanton

Aerodyne Research, Inc
45 Manning Road
Billerica, MA 01821

December 1983

Scientific Report No. 1

APPROVED FOR PUBLIC RELEASE; DISTRIBUTION UNLIMITED

DTIC FILE COPY

DTIC
ELECTE
MAR 1 1986
S E D

AIR FORCE GEOPHYSICS LABORATORY
AIR FORCE SYSTEMS COMMAND
UNITED STATES AIR FORCE
HANSCOM AIR FORCE BASE, MASSACHUSETTS 01731

86 3 1 013

This report has been reviewed by the ESD Public Affairs Office (PA) and is releasable to the National Technical Information Service (NTIS).

This technical report has been reviewed and is approved for publication

Edmond Murad

EDMOND MURAD
Contract Manager

Rocco Narcisi

ROCCO S. NARCISI
Branch Chief
Ionospheric Disturbances and Modifications Branch

FOR THE COMMANDER

Robert A. Skrivanek

ROBERT A. SKRIVANEK
Acting Division Director
Ionospheric Physics Division

Qualified requestors may obtain additional copies from the Defense Technical Information Center. All others should apply to the National Technical Information Service.

If your address has changed, or if you wish to be removed from the mailing list, or if the addressee is no longer employed by your organization, please notify AFGL/DAA, Hanscom AFB, MA 01731. This will assist us in maintaining a current mailing list.

Do not return copies of this report unless contractual obligations or notices on a specific document requires that it be returned.

UNCLASSIFIED

SECURITY CLASSIFICATION OF THIS PAGE (When Data Entered)

REPORT DOCUMENTATION PAGE		READ INSTRUCTIONS BEFORE COMPLETING FORM
1. REPORT NUMBER AFGL-TR-84-0056	2. GOVT ACCESSION NO. AD-A165 221	3. RECIPIENT'S CATALOG NUMBER
4. TITLE (and Subtitle) A Study of Atmospheric Reactions of Neutral Sodium Species and Other Metals of Meteoric Origin		5. TYPE OF REPORT & PERIOD COVERED Scientific Report No. 1 6. PERFORMING ORG. REPORT NUMBER ARI-RR-385
7. AUTHOR(s) J.A. Silver, M.S. Zahniser, C.E. Kolb, and A.C. Stanton		8. CONTRACT OR GRANT NUMBER(s) F19628-83-C-0010
9. PERFORMING ORGANIZATION NAME AND ADDRESS Aerodyne Research, Inc. 45 Manning Road Billerica, MA 01821		10. PROGRAM ELEMENT, PROJECT, TASK AREA & WORK UNIT NUMBERS 61102F 2310G3AY
11. CONTROLLING OFFICE NAME AND ADDRESS Air Force Geophysics Laboratory Hanscom AFB, Massachusetts 01731 Contract Manager: Charles Gallagher/LID		12. REPORT DATE December 1983 13. NUMBER OF PAGES 64
14. MONITORING AGENCY NAME & ADDRESS(if different from Controlling Office)		15. SECURITY CLASS. (of this report) Unclassified 15a. DECLASSIFICATION/DOWNGRADING SCHEDULE

16. DISTRIBUTION STATEMENT (of this Report)

APPROVED FOR PUBLIC RELEASE; DISTRIBUTION UNLIMITED

17. DISTRIBUTION STATEMENT (of the abstract entered in Block 20, if different from Report)

18. SUPPLEMENTARY NOTES

19. KEY WORDS (Continue on reverse side if necessary and identify by block number)

reaction rates
atomic sodium
atomic potassium
oxygen
diffusion
sodium hydroxide
hydrochloric acid

20. ABSTRACT (Continue on reverse side if necessary and identify by block number)

The reactions of metallic species introduced into the atmosphere by meteor ablation may play a significant role in mesospheric and stratospheric chemistry. Rate constants for the recombination reactions of alkali atoms with molecular oxygen, $K + O_2 + M \rightarrow KO_2 + M$ and $Na + O_2 + M \rightarrow NaO_2 + M$, have been measured as a function of temperature from 300 to 700 K using a fast flow reactor. Laser induced fluorescence is used to monitor the disappearance of Na or K as a

DD FORM 1 JAN 73 1473 EDITION OF 1 NOV 65 IS OBSOLETE
S/N 0102-LF-014-6601

UNCLASSIFIED
SECURITY CLASSIFICATION OF THIS PAGE (When Data Entered)

function of O_2 and M. The reactions are studied in their low pressure third order limit from 1 to 7 torr total pressure with N_2, He, and Ar as third bodies. The rate constants are found to have the expected negative temperature dependence. The values for k (Na + O_2 + M) are $(1.9 \pm 0.4) \times 10^{-30} (T/300)^{-1.1\pm0.5}$ with M = N_2, $(1.4 \pm 0.3) \times 10^{-30} (T/300)^{-0.9\pm0.5}$ with M = He, and $(1.2 \pm 0.3) \times 10^{-30}$ at T = 324 K with M = Ar, all in units of molecules^{-2} cm^6 s^{-1}. The values for the corresponding reactions with potassium are larger than those for sodium with k (K + O_2 + M) = $(5.4 \pm 0.2) \times 10^{-30} (T/300)^{-0.56\pm0.14}$ with M = N_2, $(2.0 \pm 0.5) \times 10^{-30} (T/300)^{-0.9\pm0.5}$ with M = He, and $(3.5 \pm 1.0) \times 10^{-30}$ at T = 300 K with M = Ar. The results are compared with other recent measurements from flame and flash photolysis studies and with theoretical expectations based on an energy transfer RRKM mechanism for the NaO_2^* activated complex.

It has been suggested that the reaction of NaOH with HCl might affect the concentration of odd chlorine, thus having an impact on the ozone balance. This report also describes the first measurement of this reaction rate constant. At 308 K, we find that k = $(2.8 \pm 0.9) \times 10^{-10}$ cm^3 molecule^{-1} s^{-1}. As a result of the methods developed to perform this measurement, we have also determined estimates of the following room temperature rate constants in units of cm^3 molecule^{-1} s^{-1}: k(NaO + HCl → NaCl + OH) ≃ 2.8×10^{-10}, k(NaOH + H → Na + H_2O)>4×10^{-12}, k(NaCl + H → Na + HCl) ≃ $5 \times 10^{-(14\pm1)}$ and k(Na + H_2O_2)≃ 6.9×10^{-11}, where approximately 0.6 of the reactions produce NaOH + OH, with the remainder forming NaO + H_2O. The impact of these and reactions currently under investigation are discussed.

Accession For
NTIS GRA&I
DTIC TAB
A-1

TABLE OF CONTENTS

1. OBJECTIVE 1

1.1 Introduction 1

1.2 Work Forecast 6

1.3 References 7

2. TEMPERATURE DEPENDENT TERMOLECULAR REACTION RATE CONSTANTS FOR POTASSIUM AND SODIUM SUPEROXIDE FORMATION 9

Introduction 9

Experimental 12

Results and Discussion 15

Implications for Secondary Combustion Suppression 20

Oxidation of Meteor Metals in the Upper Atmosphere 21

Acknowledgements 22

References 23

3. THE GAS PHASE REACTION RATE OF SODIUM HYDROXIDE WITH HYDROCHLORIC ACID 33

Introduction 33

Experimental 36

Results 40

Na + H_2O_2 Reaction 40

NaOH + HCl Reaction 41

Detector Corrections and Modeling 42

Discussion 45

Acknowledgements 47

References 49

1. OBJECTIVE

1.1 Introduction

Metallic elements volatilized during meteor entry into the Earth's upper atmosphere play a significant role in the structure of the D and E regions of the ionosphere,[1-2] and, at least in the case of sodium, the visible day and nightglow emissions from the mesosphere and lower thermosphere.[3-5] Recently, it was suggested that sodium and other meteor metals may be important in stratospheric chemistry by affecting ozone reduction by the catalytic chlorine cycle.[6-8]

The influx of meteor metals into the upper atmosphere has been estimated[9] to be 3.5×10^6 kg yr^{-1}, with a sodium abundance of 2% leading to a calculated sodium flux of 1.2×10^4 atoms cm^{-2} s^{-1}. Other estimates of sodium flux run as high as 2×10^4 cm^{-2} s^{-1}.[10] The flux of other metallic species such as Mg, Ca, Al, Si and Fe will be as much as 10 times higher and speculative concerns about their influence on upper atmospheric homogeneous and heterogeneous chemistry have been published.[1-2,7-8,10]

Unfortunately, all attempts to model the role of volatilized meteor metals (particularly sodium) in the mesosphere and stratosphere[3-4,7,19-15] have suffered from an almost total lack of measured rate constants. All such models start with the oxidation of sodium or other metallic species in reaction with atmospheric O, O_2, or O_3. Until 1982, the only measured chemical rate constants available for any meteor metal oxidation reactions were the three body recombination reactions of alkali atoms (Na, K) with O_2[16-18]

$$\text{Na or K} + O_2 + M \rightarrow NaO_2 \text{ or } KO_2 + M \quad . \tag{1}$$

Flame studies by Hynes et al[17] and direct measurements at 724 and 844 K by Husain and Plane[16] showed that this reaction rate is 1000 times faster than

previously believed.[19-20] Recent direct flow tube measurements[18] in our laboratory have extended these results from 700 K down to 300 K, and show that the reaction rates vary inversely with temperature, and confirm the larger values for the rate constants.

As an indication of the effect that the availability of chemical rate data has on aeronomic modeling studies, consider the theoretical calculation of several important sodium oxidation reaction rate constants:

$$Na + O_3 \rightarrow NaO + O_2 \quad (2)$$

$$NaO + O \rightarrow Na + O_2 \quad (3)$$

and

$$NaO + O_3 \rightarrow \text{Products} \quad (4)$$

performed at Aerodyne Research, Inc.[21] The adoption of realistic values for just these three rate constants has led to a major revision in the understanding of the structure of the mesospheric sodium layer,[22] the magnitude of the sodium D line nightglow,[5,21] and the understanding of long-lived luminous meteor trails.[8,21]

From the recent modeling work[7-8,10,13,21-22] and comparison of these models with atmospheric measurements,[12,14-15] neutral sodium is believed to be transformed via a series of chemical reactions involving NaO, NaO_2, and NaOH. A survey of the relevant literature[6-8,10,13] provides a fairly complete list of possible neutral sodium reactions of importance. These are listed in Table 1, in four groups, which to some extent, reflect the sequence of events from the introduction of neutral sodium at 110 km altitude to its disappearance near 70 km. Also listed are reaction enthalpies, with associated uncertainties.

Table 1 - Atmospheric Reactions of Neutral Sodium Species

		$-\Delta H^\circ_r$ (kJ mol^{-1})
I. Sodium Atom Reactions		
$Na + O_2 \xrightarrow{M}$	NaO_2	163 ±21
$Na + O_3 \rightarrow$	$NaO + O_2$	167 ±42
$Na + HO_2 \rightarrow$	$NaOH + O$	77 ±15
	$NaH + O_2$	4 ±21
	$NaO + OH$	
$Na + O \xrightarrow{M}$	NaO	273 ±42
II. Sodium Oxide Reactions		
$NaO + O_3 \rightarrow$	$NaO_2 + O_2$	282 ±47
	$Na + 2O_2$	119 ±42
$NaO + H_2O \rightarrow$	$NaOH + OH$	1 ±44
$NaO + H_2 \rightarrow$	$NaOH + H$	64 ±44
$NaO + CH_4 \rightarrow$	$NaOH + CH_3$	61 ±44
$NaO + HCl \rightarrow$	$NaCl + OH$	134 ±42
$NaO + O \rightarrow$	$Na + O_2$	225 ±42
$NaO + HO_2 \rightarrow$	$NaOH + O_2$	303 ±44
$NaO + H \rightarrow$	$Na + OH$	155 ±42
$NaO + ClO \rightarrow$	$NaOCl + O$	
$NaO_2 + HCl \rightarrow$	$NaCl + HO_2$	13 ±23
$NaO_2 + Cl \rightarrow$	$NaCl + O_2$	247 ±21
$NaO_2 + ClO \rightarrow$	$NaCl + O_3$	84 ±21
$NaO_2 + H_2 \rightarrow$	$NaOH + OH$	103 ±24
	$NaO + H_2O$	103 ±47
$NaO_2 + O \rightarrow$	$NaO + O_2$	110 ±47
$NaO_2 + OH \rightarrow$	$NaOH + O_2$	181 ±24
$NaO_2 + H \rightarrow$	$NaOH + O$	111 ±24
	$Na + HO_2$	34 ±23
III. Sodium Hydroxide Reactions		
$NaOH + HCl \rightarrow$	$NaCl + H_2O$	133 ±13
$NaOH + Cl \rightarrow$	$NaCl + OH$	67 ±13
$NaOH + ClO \rightarrow$	$NaCl + HO_2$	63 ±15
$NaOH + H \rightarrow$	$Na + H_2O$	154 ±13
$NaOH + CO_2 \xrightarrow{M}$	$NaHCO_3$	
$NaOH + HNO_3 \rightarrow$	$NaNO_3 + H_2O$	
$NaHCO_3 + HCl \rightarrow$	$NaCl +$ Products	
IV. Photolysis Reactions		
$NaOH + h\nu \rightarrow$	$Na + OH$	
$NaO + h\nu \rightarrow$	$Na + O$	
$NaO_2 + h\nu \rightarrow$	$Na + O_2$	
$NaCl + h\nu \rightarrow$	$Na + Cl$	

The main removal mechanisms of sodium are by reaction with O_2 or O_3, the latter reaction used by Chapman[23] to describe the Na nightglow. The recent rate measurements of reaction (1) however, lead us to believe that below 80 km most of the Na is converted to NaO_2.

The fate of NaO_2, however, is uncertain. Recent measurements by Figger et al[24] and flame studies by Hynes et al[17] imply that the Na-O_2 bond strength is much weaker than previously believed, with a value of ca. 163 kJ mol^{-1}. As a result, NaO_2 will react exothermically with atomic oxygen to produce NaO. Sodium oxide can react either with ozone to reform NaO_2 or react with water to produce NaOH.

$$NaO_2 + O \rightarrow NaO + O_2 \qquad (5)$$

$$NaO + O_3 \rightarrow NaO_2 + O_2 \qquad (6)$$

$$NaO + H_2O \rightarrow NaOH + OH \qquad (7)$$

Unfortunately, none of these rates has been measured, leading the various modelers to speculate on the importance of each.[10,12-15] As shown by Sze et al,[13] the predominant alkali species below 70 km may be NaO, NaO_2, and/or NaOH, depending on ones choice for k_5, k_6, and k_7.

In a recent paper by Murad et al,[8] it was proposed that the reactions of metal hydroxides and superoxides with chlorine compounds between 40 and 70 km may have an impact on the depletion of stratospheric ozone. In the case of sodium, the exothermic bimolecular reactions

$$NaOH + HCl \rightarrow NaCl + H_2O \quad , \tag{8}$$

$$NaOH + ClO \rightarrow NaCl + HO_2 \quad , \tag{9}$$

$$NaOH + Cl \rightarrow NaCl + OH \tag{10}$$

$$NaO_2 + HCl \rightarrow NaCl + HO_2 , \tag{11}$$

$$NaO_2 + ClO \rightarrow NaCl + O_3 \quad , \tag{12}$$

$$NaO_2 + Cl \rightarrow NaCl + O_2 \tag{13}$$

might be expected to proceed rapidly and act as a sink for Cl, given that NaCl can readily polymerize and condense via heterogeneous nucleation.[8] Murad et al calculated that if the reaction rate of these sodium species with HCl were $\sim 10^{-11}$ cm^3 $molecule^{-1}$ s^{-1}, they might be comparable to the major Cl regeneration mechanism,

$$OH + HCl \rightarrow Cl + H_2O \quad . \tag{14}$$

While previously published studies have viewed NaCl as a potential sink for stratospheric chlorine,[7-8] more recent analyses by F.S. Rowland[25] indicate that photolysis of NaCl may in fact release free Cl. Given the potentially large J values (atmospheric photolysis rate) for this process,[25-26] reactions (8)-(13) could effectively supplement, rather than remove, reaction (14) as a release mechanism for Cl from the inactive HCl stratospheric reservoir and thereby determine the extent to which ozone might be depleted by chlorine compounds in the stratosphere. However, to fully understand the role of alkali species in the stratosphere one must also consider the effects of NaO_2 and NaOH photodissociation on those processes.[13,27]

The objective of this work is to provide direct experimental measurements of these key rate constants. Obtaining accurate reaction rates for the sodium atmospheric system will enable more accurate modeling of the sodium emission and density profiles. Once this is completed, these results can be extended toward the larger goal of understanding the chemistry of the more abundant meteor metals.

The work during this past year has concentrated on two reactions, Na (and K) + O_2 + M, and NaOH + HCl. Experimental determinations of their rate constants are presented in the next two sections of this report.

1.2 Work Forecast

During the next year of this program, we will continue our examination of the chemistry of alkali metals in the mesosphere and upper stratosphere. Our initial work will be the measurement of the rate constant for Na with ozone. This will also provide us with a source of NaO, with which we will measure the very important rate constant for the reaction of NaO with H_2O. Detection techniques for NaO have been developed during the first year of this program. We also plan, later in the year, to begin investigating the chemistry of NaO_2.

1.3 References

1. Murad, E., J. Geophys. Res. 83, 5525 (1978).

2. Brown, T.L., Chem. Rev. 73, 645 (1973).

3. Blamont, J.E. and Donahue, T.M., J. Geophys. Res. 69, 4093 (1964).

4. Hunten, D.M., Space Sci. Rev. 6, 493 (1967).

5. a) Kirchhoff, V.W.J.H., Clemesha, B.R., and Simonich, D.M., J. Geophys. Res. 84, 1323 (1979);
   b) Bates, D.R. and Ojha, P.C., Nature 286, 790 (1980).

6. Ferguson, E.E., Geophys. Res. Lett. 5, 1035 (1978).

7. Murad, E. and Swider, W., Geophys. Res. Lett. 6, 929 (1979).

8. Murad, E., Swider, W., and Benson, S.W., Nature 289, 273 (1981).

9. Richter, E.S. and Sechrist, C.F., Jr., J. Atmos. and Terres. Phys. 41, 579 (1979), Geophys. Res. Lett. 6, 183 (1979).

10. Liu, S.C. and Reid, G.C., Geophys. Res. Lett. 6, 283 (1979).

11. a) Baggaley, W.J., Nature 257, 567 (1975);
    b) Baggaley, W.J., Nature 267, 376 (1977);
    c) Hapgood, M.A., Nature 286, 582 (1980.

12. Kirchhoff, V.W.J.H., Clemesha, B.R., and Simonich, D.M., J. Geophys. Res. 86, 6892 (1981).

13. Sze, N.D., Ko, M.K.W., Swider, W., and Murad, E., Geophys. Res. Lett. 9, 1187 (1982).

14. Kirchhoff, V.W.J.H., Geophys. Res. Lett. 10, 721 (1983).

15. Thomas, L., Isherwood, M.C., and Bowman, M.R., J. Atm. Terrestrial Phys. 45, 587 (1983).

16. Husain, D. and Plane, J.M.C., J. Chem. Soc. Far. Trans. 2, 78, 163 (1982).

17. Hynes, A.J., Steinberg, M., and Schofield, K., Submitted for publication in J. Chem. Phys.

18. Silver, J.A., Zahniser, M.S., Stanton, A.C., and Kolb, C.E., manuscript in preparation.

19. Carabetta, R. and Kaskan, W.E., J. Phys. Chem. 72, 2483 (1968).

20. McEwan, M.J. and Phillips, L.F., Trans. Faraday Soc. 62, 717 (1966).

21. Kolb, C.E. and Elgin, J.B., Nature 263, 488 (1976).

22. Simonich, D.M., Clemesha, B.R., and Kirchoff, V.W.J.H., J. Geophys. Res. 84, 1543 (1979).

23. Chapman, S., Astrophys. J. 90, 309 (1939).

24. Figger, H., Schrepp, W. and Zhu, Xu-hui, J. Chem. Phys. 79, 1 (1983).

25. Rowland, F.S. and Rogers, P.J., Proc. Natl. Acad. Sci. USA 79 (1982).

26. Davidovits, P. and Brodhead, D.C., J. Chem. Phys. 46, 2968 (1967).

27. Rowland, F.S. and Makide, Y., Geophys. Res. Lett. 9, 473 (1982).

2. TEMPERATURE DEPENDENT TERMOLECULAR REACTION RATE CONSTANTS FOR POTASSIUM AND SODIUM SUPEROXIDE FORMATION

(To be submitted to the 20th Symposium (International) On Combustion.)

INTRODUCTION

The chemistry of alkali metals in flames commands our attention for both scholarly and practical reasons. From a scientific standpoint reactions of alkali atoms, with their single valence electron, form a natural test bed to extend our theoretical understanding honed on reactions of atomic hydrogen. Furthermore, the low ionization potentials of alkali atoms open the possibility of electron transfer reaction mechanisms and allow determination of the role of ionic potential surfaces in reaction dynamics. Finally, incredibly sensitive methods of detecting alkali atoms, including hot wire surface ionization, laser induced resonance fluorescence, and laser induced resonance ionization now allow the design of elegant experimental studies for environments ranging from molecular beams to high pressure flames.

From a practical standpoint, the alkali chemistry of flames is focused primarily on understanding and utilizing the flame suppression properties of alkali additives. Laboratory studies[1-3] in the 1960's and early 1970's clearly indicated the critical nature of the reaction:

$$KOH\ (NaOH) + H \rightleftarrows K\ (Na) + H_2O \qquad (1)$$

as the major radical scavenging reaction responsible for alkali flame suppression. Since then, detailed computer studies of alkali suppression of secondary muzzle flash[4,5] and of rocket exhaust plume afterburning[6,7] have confirmed the importance of reaction (1), but have also indicated that secondary formation of alkali superoxides:

$$K\ (Na) + O_2 + M \rightarrow KO_2\ (NaO_2) + M \qquad (2)$$

followed by potential superoxide reactions such as:

$$KO_2\ (NaO_2) + H \begin{cases} \rightarrow K(Na) + HO_2 \\ \rightarrow KO(NaO) + OH \end{cases} \qquad (3)$$

$$KO_2\ (NaO2) + H_2 \begin{cases} \rightarrow KOH\ (NaOH) + OH \\ \rightarrow KO\ (NaO) + HO_2 \end{cases} \qquad (4)$$

$$KO_2\ (NaO_2) + OH \rightarrow KOH\ (NaOH) + O_2 \qquad (5)$$

can significantly affect the degree of alkali suppression in many circumstances.

However, for all the intrinsic theoretical and experimental interest in alkali reactions, our understanding of the gas phase oxidation chemistry of alkali atoms has only recently progressed, first back to, and then beyond the level gained in the 1930's in pioneering sodium diffusion flame studies by Haber and Sachsse[8] and Bawn and Evans.[9] While these low pressure studies of reaction (2) showed it proceeded with a termolecular rate constant in excess of 10^{-30} cm^3 s^{-1},[8,9] subsequent work (primarily in the mid 1960's) using flame photometric methods by Kaskan[10,11] and McEwan and Phillips[12,13] indicated much lower MO_2 formation rates (M=Na,K)[10,11,12] as well as relatively high dissociation energies for the $M-O_2$ bond (M=Na,Li).[12,13]

Analyses of thermochemical cycles by Herm and Herschbach[14] and Alexander[15] clearly indicated that the values of $M-O_2$ bonds deduced from flame photometric data by McEwan and Phillips were greatly overestimated. This was recently confirmed by Figger and co-workers who analyzed observations of chemiluminescence between crossed molecular beams of alkali dimers and molecular oxygen to yield alkali superoxide bond energies.[16] Reinterpretation of the earlier flame experiments[17] as well as newly performed flame studies are also consistent with lower alkali superoxide bond energies.[18]

The low sodium and potassium termolecular reaction rates deduced from the flame photometry studies[10,11,12] are also incorrect. Recently published flash photolysis studies over limited temperature ranges for Li (393 and 463 K),[19] Cs (323 K),[20] Na (724 and 844 K),[21] and K (753 and 853 K),[22] as well as flame photometry studies for Na[18], all clearly show fast termolecular rates for alkali superoxide formation.

In this paper we report termolecular rate constants for superoxide formation of sodium and potassium over a much wider temperature range than previously available, yielding the first clear, direct measurement of the temperature dependence of these processes. Third body dependencies are illustrated by separate measurements for N_2, He and Ar. These measurements were made in Aerodyne's high temperature, fast flow reactor[23] utilizing laser induced resonance fluorescence detection of atomic alkali species. A discussion of these results in terms of their importance in testing termolecular association reaction theory and for the more applied concerns of secondary combustion suppression and the oxidation of meteor deposited metals in the upper atmosphere will also be presented.

EXPERIMENTAL

The high temperature fast flow reactor used in these experiments has been described in detail previously[23] and is shown in Fig. 1 in the configuration used in this study. Briefly, a 7.26 cm diameter, 120 cm long alumina tube is heated with Kanthal resistance heaters capable of maintaining uniform temperatures in the reaction zone. The helium, argon or nitrogen carrier gas enters the flow tube through two mullite multichannel arrays which both preheat and laminarize the flow upstream of the reaction zone. A sufficient distance (20 cm) is allowed downstream of these arrays for the carrier gas to develop a parabolic flow profile before reaching the reaction zone. The gas is pumped by a 450 liter s^{-1} Roots blower and mechanical fore pump combination. Linear flow velocities from 450 to 1900 cm s^{-1} are used in the present experiments. Carrier gas flow rates from 40 to 400 STP cm^3 s^{-1} are measured with calibrated rotameters. Total pressures in the range from 1 to 8 torr are measured with a capacitance manometer at the downstream end of the reaction zone. Gas temperatures are obtained with a chromel-alumel thermocouple which is movable throughout the reaction zone. Although the apparatus is capable of temperatures up to 1500 K, experimental considerations as described below limited the upper temperature to 700 K for these studies.

Alkali atoms are generated by heating the pure metal in a 25 mm diameter cylindrical silver plated monel oven to a temperature sufficient to obtain a vapor pressure of 10^{-6} to 10^{-4} torr within the oven. The oven is mounted on the end of a movable 13 mm od alumina tube concentric to the main flow tube. The vapor is entrained in a flow of carrier gas and introduced into the flow tube in one of two configurations. For the kinetic measurements with O_2, the oven is placed at a fixed position upstream of the multichannel arrays and the alkali vapor is introduced into the main flow through a 10 cm length of 19 mm o.d. silver tubing which passes through the center of the arrays. In the second configuration, the oven is placed downstream of the arrays and is movable throughout the reaction zone to determine the loss of alkali atoms on

the reactor walls. The oven temperature is controlled with resistive heating elements independent of the flow tube heaters. Initial alkali atom concentrations in the reaction zone are maintained at less than 10^{10} atoms cm^{-3} by adjusting the oven temperature and the carrier gas flow rate through the oven.

The alkali atoms are detected by laser induced fluorescence at the downstream end of the flow tube. A Molectron DL14 nitrogen pumped dye laser is used to excite the $4s^2S_{1/2} \rightarrow 5p^2P_{3/2}$ transition at 404.4 nm for potassium or the $3s\ ^2S_{1/2} \rightarrow 3p\ ^2P_{3/2}$ transition at 589.0 nm for sodium. Fluorescence is collected using a gated phototube and a computer controlled data acquisition system.[23] The signals are averaged over 100 laser pulses after subtracting for nonfluorescent background contributions and normalizing for pulse to pulse fluctuations in laser intensity. Although no direct calibration of the fluorescence signal was attempted,. estimates of sensitivity from known phototube and integrator response, measured laser power, and atomic transition probabilities indicate a detection limit for Na of 10^4 cm^{-3} and for K of 10^6 cm^{-3} using these transitions.

Molecular oxygen is added through a movable loop injector at distances from 10 to 60 cm upstream of the detection region. O_2 flow rates are measured with a calibrated thermal conductivity mass flow meter. The kinetic measurements are conducted under pseudo-first order conditions with $2 \times 10^{14} < [O_2] < 7 \times 10^{15}$ cm^{-3}, in large excess compared to the alkali metal atom concentration, yet always <5% of the total gas concentration. First order rate constants are determined for a fixed O_2 concentration by recording the change in alkali atom concentration as a function of O_2 injector distance.

Corrections for both axial and radial diffusion and wall removal are made using the procedure outlined by Brown.[24] This method is based on a numerical solution of the continuity equation including diffusion, first order chemical reaction and wall removal in a cylindrical tube with fully developed laminar flow. A multiplicative correction factor, obtained for each set of experimental conditions, is used to relate the observed decay to the true

first order rate constant. This correction factor is dependent on the wall removal rate constant, k_w, and the binary diffusion coefficient for the alkali atom in the carrier gas. Values for k_w are determined in separate experiments at each pressure and temperature by observing the change in atom concentration at the detection point while varying the source oven position. The loss of atoms to the wall was found to be diffusion limited for all the conditions used in this study, implying a surface accommodation coefficient $\gamma > 0.1$. The observed wall loss rate under these conditions may therefore be used to determine the diffusion coefficient. This procedure, based on Brown's[24] approach for obtaining solutions to the transport equation, is given in more detail elsewhere.[25] The resulting values for D (1 atm), which are used in the diffusion corrections for this study, are given in Table I. The correction factors obtained by this method were in the range k_{true}/k_{obs} from 1.52 to 1.86, with most lying between 1.60 and 1.65. Under the flow conditions of these experiments, the ratio of reaction to diffusion times is not unlike those encountered in ion-molecule reactions,[26] which also exhibit correction factors on the order of 1.6.

Table I. Binary Diffusion Coefficients for Na and K in He and N_2

COMPONENTS	D ($cm^2\ s^{-1}$ at 1 atm)
Na, He	$1.2 \times 10^{-5}\ T^{1.9}$
Na, N_2	$1.7 \times 10^{-6}\ T^{2.0}$
K, He	$3.1 \times 10^{-5}\ T^{1.7}$
K, N_2	$3.8 \times 10^{-5}\ T^{1.6}$

RESULTS AND DISCUSSION

Reaction rate constants of atomic sodium with O_2 were measured over the temperature range of 320 - 698 K for nitrogen as the third body collision partner, and over the range of 309 - 473 K in helium; for potassium, the corresponding temperature ranges were 308 - 720 K and 296 - 520 K, respectively. Room temperature measurements were also made in argon for both Na and K. Pressures encompassed at each temperature range from 1 to between 5 and 8 torr. Above 700 K, no reliable decays could be measured, because alkali atoms which had accumulated on the walls at lower temperatures began to effuse into the flow, interfering with the rate measurements.

Using the data for Na + O_2 + (He) as an example, we see in Fig. 2 that the first-order (logarithmic) decays of signal with reaction time are linear for over a factor of 100. Plots of a series of first-order rate constants (corrected for wall and diffusional effects) versus $[O_2]$ are illustrated in Fig. 3. Second-order rate constants derived from these are then plotted vs. total number density (Fig. 4). The third-order rate constants are then determined as the slopes of these plots. In most cases, these lines intersect the origin to within the statistical uncertainties of the fit. For Na + O_2 + (N_2), a finite intercept is observed at all temperatures, although it never exceeds 4×10^{-13} cm^3 s^{-1}. This may be attributed to the fact that the oxygen concentration reached 10-15% of the total number density in the low pressure runs for this system. If $k^{III}(M = O_2) > k^{III}(M = N_2)$, then what is reported as $k^{II}(N_2)$ would be overestimated, resulting in a small finite intercept and a value for $k^{III}(Na + O_2 + N_2)$ that is ~ 15% low. An alternating explanation sometimes given for such behavior is that the wall acts as a stabilizing third body and adds a pressure independent component to k^{II}. However, this explanation would appear unlikely in these experiments given the near unit efficiency for wall removal of all alkali species.

The three-body association rate constants as a function of temperature for various third body collision partners are shown for sodium in Fig. 5 and

for potassium in Fig. 6. The data can be described by an expression of the form $k^{III}(T) = AT^{-n}$. The results of nonlinear least-square fits to this function are found in Tables II and III. For sodium in helium and nitrogen, and for potassium in helium, a simple T^{-1} representation could also be used. However, the results for potassium in nitrogen show a weaker temperature dependence, best represented by $T^{-(0.56 \pm 0.14)}$.

The experimental values for these rate constants are listed in Tables II and III. The expressed total experimental uncertainties, including allowance for systematic errors, can be estimated as the square root of the sum of the squared individual uncertainties due to a) flow velocity, temperature, pressure, and concentration calibration factors, 5%, b) the precision in determining the coefficient A in the expression for $k^{III}(T)$, 17%, and c) the uncertainty in the correction of observed first-order decays for wall removal and diffusional effects, 10%.

Tables II and III also contain a comparison with other determinations of k_2. Husain and Plane[21,22] used a flash photolysis system to generate alkali atoms from KI and NaI and followed the decay of K and Na by atomic resonance absorption. They observed no temperature dependence over their limited temperature range (724 K and 844 K) for the Na + O_2 + M reaction. A substantially larger variation with temperature was obtained for their K + O_2 + M study although they arbitrarily fit their data to a T^{-1} dependence. The agreement between their values and the slightly extrapolated temperature dependent rate constants for both reactions from this work is satisfactory, especially considering the very different methods employed. This comparison is shown in Figs. 5 and 6.

Hynes et al.[18] have studied the Na + O_2 + M reaction in experiments using laser induced fluorescence to measure Na and OH profiles under fuel lean conditions in $H_2/O_2/N_2$ flames. A detailed kinetic model assuming reasonable values for rate constants for the reactions interconnecting the species Na, NaO_2, NaO and NaOH is used to determine the best fit to the observations. Their "best fit" value of k(Na + O_2 + M), for which they state an accuracy of

a factor of two, is reported assuming a T^{-1} temperature dependence. As shown in Fig. 5, their value is lower by about a factor of 4 compared to the extrapolated value from this work. Hynes et al.[18] also explain the discrepancy between their result and the earlier flame studies,[10-12] which obtained a lower value for k(Na + O_2 + M) by nearly three orders of magnitude, as being due to the neglect of the effects of secondary reactions in the interpretation of the earlier studies. A similar explanation has been proposed by Jensen.[17]

The much earlier diffusion flame studies[8,9] correctly identified the Na + O_2 + M reaction to be fast for a three body process. The later and more extensive study by Bawn and Evans[9] obtained a value at 533 K which is higher by a factor of 3 than this study. They also observed a fall-off behavior for their second order rate constant with pressure above about 10 torr and present their results in terms of an energy transfer mechanism using a Lindemann-type expression to interpret their data. This fall-off behavior was not observed by Husain and Plane[21] who show linear plots of k_2^{II} versus pressure from 25 to 150 torr. Their effective bimolecular rate at 150 torr and 724 K for the Na + O_2 + (N_2) reaction of 2.2×10^{-12} cm^3 s^{-1} is nearly equal to the high pressure limit inferred by Bawn and Evans of 3×10^{-12} cm^3 s^{-1}. It thus appears that the pressure dependence observed by Bawn and Evans may have been an artifact of their experimental diffusion flame technique. No curvature was observed in our lower pressure $P \leq 7$ torr conditions of this study as shown in Fig. 4, and, under these conditions, the recombination reaction appears to be in its low pressure, third order, limit.

In this limit, the recombination rate constant can best be calculated using unimolecular rate theory[27], in which second-order rate constants for unimolecular decomposition are related through the equilibrium constant to the third order (low pressure) association rate constants. The unimolecular rate constants are obtained using simplified equations of Troe based on RRKM theory.[28,29] The recombination rate constant can be expressed as the product of a strong collision rate constant $k_{rec,o}^{sc}$ and a weak collision deactivation efficiency term β_c,

$$k_{rec} = k^{sc}_{rec,o}\,\beta_c \qquad (6)$$

In effect, β_c is a term expressing the efficiency by which $(NaO_2)^*$ is stabilized upon collision. In the absence of detailed state-to-state energy transfer rates, β_c is an adjustable parameter which depends on the average change in internal energy of the transition state complex per collision, $\langle\Delta E\rangle$, so that

$$\frac{\beta_c}{1-\beta_c^{1/2}} = \frac{\langle\Delta E\rangle}{F_E RT} \quad . \qquad (7)$$

F_E is a correction term for the energy dependence of the density of states in the transition complex. Using structural data from Ref. 15, and deriving $\Delta H_f^{298} = -55.7$ kJ mole^{-1} from a value of 163 kJ mole^{-1} for the Na-O_2 bond energy,[18] Patrick and Golden have calculated k^{sc}_{rec} for Na + O_2 + (He) at 300 and 700 K.[30] The computations result in $k^{sc}_{rec,o}$ (300 K) = 7.8×10^{-30} cm^6 molecule^{-1} s^{-1} for M = He. Thus, a value of $\beta_c = 0.18$ is required to reproduce the experimental result. The average energy transferred per collision is 0.8 kJ mole^{-1}. At 700 K, $k^{sc}_{rec,o} = 4.2 \times 10^{-30}$ cm^6 molecule^{-2} s^{-1}, suggesting a value of $\beta_c = 0.09$ if $\langle\Delta E\rangle$ is assumed to be independent of temperature. Extrapolation of the experimental value for helium to 700 K results in an observed $\beta_c = 0.14$, in good agreement, considering the simplified assumptions of this approach.

This unimolecular approach has been shown to be fairly reliable in calculating termolecular association rate constants for a variety of species.[27,29] The values of β_c for M = N_2 and Ar tend to lie in the range of 0.1 - 0.5. The calculations for Na + O_2 in helium agree quite well with these numbers, given that one might expect helium to be somewhat less efficient than N_2 in quenching the excited intermediate. For the similar reaction H + O_2 + (N_2), the calculations also perform well, giving β_c =

0.08, even though the rate constant for this reaction, 5.9×10^{-32} cm^6 s^{-1} at 300 K[31], is approximately 30 times slower than the corresponding sodium reaction.

In extrapolating our measured rate constants to higher pressures, it is important to understand the fall-off behavior as the reaction mechanism goes from its low pressure third order limit to its high pressure second order limit. A method for calculating the fall-off parameter based on RRKM theory has been developed by Luther and Troe.[32] Using their approach, the bimolecular rate constant in the transition region may be calculated as[27,31]

$$k^{II} = \frac{k_\infty \, k_o[M]}{k_\infty + k_o[M]} \; F^{\left\{1+\left[\log_{10}(k_o[M]/k_\infty)\right]^2\right\}^{-1}} \qquad (8)$$

where k_∞ and k_o are the high pressure and low pressure limiting rate constants, respectively. The broadening parameter, F, is dependent on the molecular structure of the adduct and typically is on the order of 0.6 for small molecules.[27] The Patrick and Golden calculation for NaO_2^* gives F = 0.5.[30]

In order to assess the fall-off behavior, the association rate k_∞ may be estimated from the dynamics of the Na + O_2 encounter. Alkali atom reactions are often described in terms of their ionic character which leads to very fast reaction rates via an electron jump mechanism.[33] Ionic forces in the alkali-oxygen associations, however, are not as dominant as in other alkali atom reaction mechanisms. Although the approaching species do adiabatically transfer from the incident covalent potential surface to an ionic surface (electron jump mechanism), the crossing distance (r_c) is relatively small as compared with alkali-halogen systems and the overall association rate is dominated by the dispersion interaction on the covalent potential surface. This is illustrated by comparing the rate constant based on the product of the mean collision velocity and the electron jump cross section (modified to

account for the dispersion and angular momentum terms in the covalent potential function),[34] to a rate constant computed solely from a close collision model,[35] in which all collisions surmounting the angular momentum barrier of a Cr^{-6} potential contribute to the rate. For Na + O_2 at 300 K, an electron jump rate constant (r_c = 2.6 Å) is 1.5 x 10^{-10} cm^3 s^{-1}, while the close collision constant is 5.9 x 10^{-10} cm^3 s^{-1}. Thus, it appears that the rate of intermediate complex formation for reaction (2) is governed by long range dispersion forces, as found in most covalent systems. Once formed, however, these intermediates are certainly (alkali)$^+O_2^-$ ion pairs.[15] In either case, the association rate constant is expected to be fast with a value for $k_\infty > 10^{-10}$ cm^3 s^{-1}.

Using a value for $k_\infty = 2 \times 10^{-10}$ cm^3 s^{-1}, Eq. (8) may be used to estimate the ratio of the observed rate constant, k_{obs}, to the true third order low pressure limit, k_o. At the maximum pressure in our studies, 7 torr, one obtains $k_{obs}/k_o = 0.91$ which indicates that our experiments are essentially in the low pressure limit. For the conditions of Husain and Plane[21] (150 torr, 724 K), this same calculation would predict k_{obs}/k_o = 0.87. For the combustion conditions with P = 760 torr T = 2000 K applicable to the Hynes et al. study[18], one obtains $k_{obs}/k_o = 0.89$. Thus, the large value for k_∞ would indicate that both of these studies are also essentially in the low pressure limit with regard to the recombination reaction.

Implications for Secondary Combustion Suppression

Solid propellants for both tactical rockets and artillery shells are frequently loaded with potassium salts (or less frequently sodium salts) to suppress the secondary combustion of the high levels of H_2 and CO found in the exhaust gases of these systems. This secondary combustion is termed afterburning for rocket systems and often leads to bright infrared[6] and visible/ultraviolet[36] signatures which are undesirable in weapons systems. Secondary combustion in gun systems is termed secondary muzzle flash, and also

produces undesirable weapons signatures as well as acoustic overpressures which can damage gun crew hearing.

Propellant designers are interested in predicting the minimum levels of potassium salt loadings necessary to produce enough KOH in the primary propellant combustion to reliably suppress secondary combustion, through reaction (1):

$$KOH\ (NaOH) + H \rightleftarrows K\ (Na) + H_2O \qquad (1)$$

when fuel rich exhaust gases mix with the atmosphere. As noted in the introduction, atomic potassium or sodium, formed either by reaction (1) or in the primary combustion process will rapidly form alkali superoxide molecules via reaction (2) at the fast rates measured in this work. Computer models of this process for both rocket exhaust afterburning[6-7] and secondary muzzle flash from guns[4-5] indicate that this process will be particularly effective in the cooler, oxygen rich regions created by substantial atmospheric dilution of exhaust products. These models also indicate that, if the alkali superoxide formed in these regions can react with residual flame radicals or molecular hydrogen via reactions (3-5), there will be a significant modification (a reduction for most reasonable rate assumptions) of the flame suppression characteristics of KOH.[5-7] The large rate constants and moderate temperature dependence measured in this work for superoxide formation increase the potential role of alkali superoxide reactions in alkali flame suppression. Efforts to provide the first experimental determination of rate constants for alkali superoxide reactions (3-5) are now underway in our laboratory.

Oxidation of Meteor Metals in the Upper Atmosphere

Atomic sodium ablated from meteors in the 90-110 km altitude region is estimated to be equivalent to a time averaged flux of over 10^4 atoms cm^{-2} sec^{-1}.[37-38] Lesser amounts of Li and K are also known to be deposited in the

same manner. Recent insight into the chemical dynamics of the upper atmospheric sodium/oxygen system[39] helped stimulate a revival of interest in the Chapman mechanism for the sodium airglow.[40] The formation of sodium superoxide through reaction (2), is now recognized as the lower altitude cut-off sink for free sodium in the 70-80 km region. The large rate constants for reaction (2) reported in this work and reference 21, coupled with accurate lidar profiles of mesospheric atomic sodium, pose a stringent test for models of diurnal and seasonal mesospheric variations,[41-43] and have caused the revision of a number of previous studies.

Below 90 km a series of chemical and photochemical reactions are thought to partition atmospheric sodium among NaO_2, NaO, NaOH, and NaCl.[37,38,41] During daylight, NaOH[44] and NaCl[45] are both predicted to undergo relatively rapid photolysis, releasing atomic sodium in the upper stratospheric and lower mesosphere. The large rate constant measured for reaction (2) in this work ensures that rapid NaO_2 formation is the fate of the overwhelming proportion of the atomic sodium thus released, and that nearly all the sodium present in gas phase molecular form is routinely cycled through the NaO_2 molecule. Efforts are now underway in our laboratory to measure reaction rates for NaO_2 with labile upper atmospheric species as well as the NaO_2 photolysis rate.

Acknowledgements

The authors would like to thank Dr. F. Kaufman for many helpful discussions, and Drs. D. Golden and R. Patrick for performing association rate calculations for sodium. The technical assistance of W. Goodwin is greatly appreciated. This work was supported by the Air Force Geophysics Laboratory under Contract Number F19628-83-C-0010, by the Army Research Office under Contract Number DAAG29-81-C-0024, and by the Chemical Manufacturers Association under Contract Number FC82-401.

REFERENCES

1. Friedman, R. and Levy, J.B.: Comb. Flame 7, 195 (1963)

2. Wolfhard, H.G., Glossman, I. and Green, L., Jr.: Prog. in Aeronautics and Astronautics 15, 419, Academic Press, 1964.

3. McHale, E.T.: Comb. Flame 24, 277 (1975)

4. Yousefian, V., May, I.W., and Heimerl, J.M., "Modeling the Occurence of Muzzle Flash in Guns": 17th JANNAF Combustion Meeting, CPIA Publication 329, Vol. 11, 125, NASA Langley Research Center, Hampton, VA, November, 1980.

5. Yousefian, V., May, I.W. and Heimerl, J.M.: "An Algebraic Criterion for the Prediction of Secondary Muzzle Flash - A Progress Report", 18th JANNAF Combustion Meeting, CPIA Publication 347, Vol. II, 63, Jet Propulsion Laboratory, Pasadena, CA, October, 1981.

6. Wormhoudt, J. and Kolb, C.E.: unpublished work, Aerodyne Research, Inc. (1980).

7. Jensen, D.E. and Jones, G.A.: Comb. Flame 41, 71 (1981)

8. Haber, F. and Sachsse, H., Z.: Physik. Chem. Bodenstein-Festband, 831 (1931)

9. Bawn, C.E.H. and Evans, A.G.: Trans. Faraday Soc. 33, 580 (1937)

10. Kaskan, W.E., Tenth Symposium (International) on Combustion, p. 41, The Combustion Institute, 1965.

11. Carabetta, R. and Kaskan, W.E.: J. Phys. Chem. 72, 2483 (1962).

12. McEwan, M.J. and Phillips, L.F.: Trans. Faraday Soc. 62, 1717 (1966).

13. Dougherty, G.J., McEwan, M.J. and Phillips, L.F.: Comb. Flame 21, 253 (1973).

14. Herm, R.R. and Hershbach, D.R.: J. Chem. Phys. 52, 5783 (1970)

15. Alexander, M.H.: J. Chem. Phys. 69, 3502 (1978).

16. Figger, H., Schrepp, W., and Zhu, X.: J. Chem. Phys. 79, 1320 (1983).

17. Jensen, D.E.: J. Chem. Soc. Faraday Trans. I 78, 2835 (1982).

18. Hynes, A.J., Steinberg, M. and Schofield, K., University of California at Santa Barbara, preprint (1983).

19. Kramer, S.D., Lehmann, B.E., Hurst, G.S., Payne, M.G., and Young, J.P.: J. Chem. Phys. 76, 3614 (1982).

20. Grossman, L.W., Hurst, G.S., Kramer, S.D., Payne, M.G., and Young, J.P.: Chem. Phys. Lett. 50, 207 (1977).

21. Husain, D. and Plane, J.M.C.: J. Chem. Soc. Faraday Trans. II, 78, 163 (1982).

22. Husain, D. and Plane, J.M.C.: J. Chem. Soc. Faraday Trans. II, 78, 1175 (1982).

23. Gersh, M.E., Silver, J.A., Zahniser, M.S., Kolb, C.E., Brown, R.G., Gozewski, C.M., Kallelis, S. and Wormhoudt, J.C.: Rev. Sci. Inst. 52, 1213 (1981).

24. Brown, R.L.: J. Res. NBS 83, 1 (1978).

25. Silver, J.A.: "Diffusion Coefficients for Gaseous Alkali Species in Helium and Nitrogen" (Manuscript in preparation).

26. Ferguson, E.E., Fehsenfeld, F.C. and Schmeltekopf, A.L.: Adv. Atomic Mol. Phys. 5, 1 (1969).

27. Patrick, R. and Golden, D.M.: Int. J. Chem. Kin. 15, 1189 (1983).

28. Troe, J.: J. Chem. Phys. 66, 4745 (1977).

29. Troe, J.: J. Chem. Phys. 66, 4758 (1977).

30. Patrick, R. and Golden, D.M., SRI International, private communication.

31. Baulch, D.L., Cox, R.A., Hampson, Jr., R.F., Kerr, J.A., Troe, J., and Watson, R.T.: J. Chem. Phys. Ref. Data 9, 295 (1980).

32. Luther, K. and Troe, J.: Seventeenth Symposium (International) on Combustion, p. 535, The Combustion Institute, 1979.

33. Levine, R.D. and Bernstein, R.B.: Molecular Reaction Dynamics, Oxford Press, 1974.

34. Gislason, E.A., Alkali Halide Vapors (P. Davidovits and D.L. McFadden, Ed.), Chap. 13, p. 415, Academic Press, 1979.

35. Johnston, H.S.: Gas Phase Reaction Rate Theory, p. 144 and 253, Ronald Press, 1966.

36. Lyons, R.B., Wormhoudt, J., and Kolb, C.E.: Prog. in Aeronaut. and Astronaut. Vol. 83, p. 128, American Inst. of Aeronaut. and Astronautics, New York, 1982.

37. Richter, E.S. and Sechrist, C.F., Jr.: J. Atmos. Terres. Phys. 41, 579 (1979); Geophys. Res. Lett. 6, 183 (1979).

38. Liu, S.C. and Reid, G.C.: Geophys. Res. Lett. 6, 283, (1979).

39. Kolb, C.E. and Elgin, J.B.: Nature 263, 488 (1976).

40. Chapman, S.: Astrophys. J. 90, 309 (1939).

41. Sze, N.D., Ko, M.C.W., Swider, W. and Murad, E.: Geophys. Res. Lett. 9, 1187 (1982).

42. Kirchhoff, V.W.J.H.: Geophys. Res. Lett. 10, 721 (1983).

43. Thomas, L., Isherwood, M.C. and Bowman, M.R.: J. Atmos. Terres. Phys. 45, 587 (1983).

44. Rowland, F.S. and Makide: Geophys. Res. Lett. 9, 473 (1982).

45. Rowland, F.S. and Rogers, P.J.: Proc. Nat. Acad. Sci., USA 79, 2737 (1982).

FIGURE CAPTIONS

Figure 1. Schematic view of the high temperature flow reactor.

Figure 2. Pseudo-first order decay of Na fluorescence signal vs. reaction distance for M = He at 309 K and 5.05 torr. $[O_2]$ = 1.09 (a), 3.36 (b), 7.29 (c), 14.3 (d), 26.6 (e); units of 10^{14} cm^{-3}.

Figure 3. Plots of first-order Na decay rates vs. $[O_2]$ for M = He and T = 309-335 K. Total pressure (torr) = 1.05 (o), 1.51 (o), 2.52 (+), 3.04 (Δ), 5.05 (∇). Each point has been corrected for the effects of diffusion and wall loss.

Figure 4. Plot of second-order Na rate constant vs. total number density for M = He at $\langle T \rangle$ = 322 K (o) and 472 K (o).

Figure 5. Plot of ln k(T) vs. ln T for the reaction Na + O_2 + M, with M = N_2 (circles), He (triangles), and Ar (square) for this work. The solid lines are least-square fits to these data. The + and x symbols represent data for M = N_2 and He, respectively from reference 21, and the dashed line (M = flame gases) is from reference 18.

Figure 6. Plot of ln k(T) vs. ln T for the reaction K + O_2 + M, with M = N_2 (circles), He (triangles), and Ar (square). The solid lines are least-square fits to these data. The + and x symbols represent data for M = N_2 and He, respectively from reference 22.

84-038

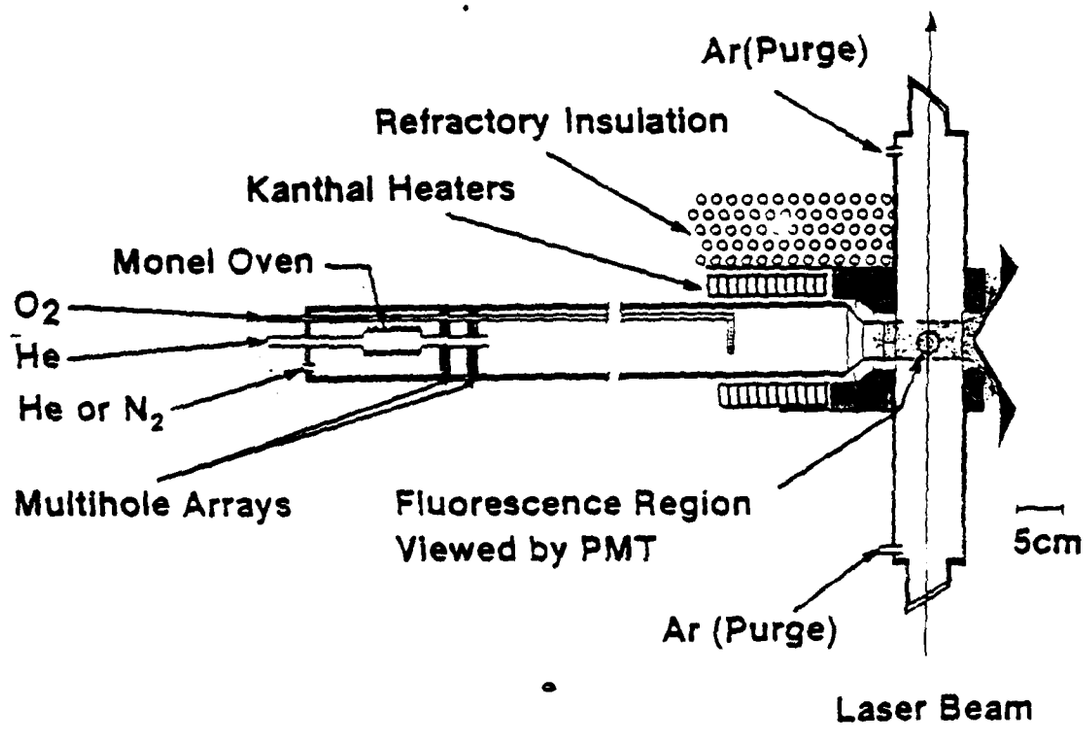


FIGURE 1

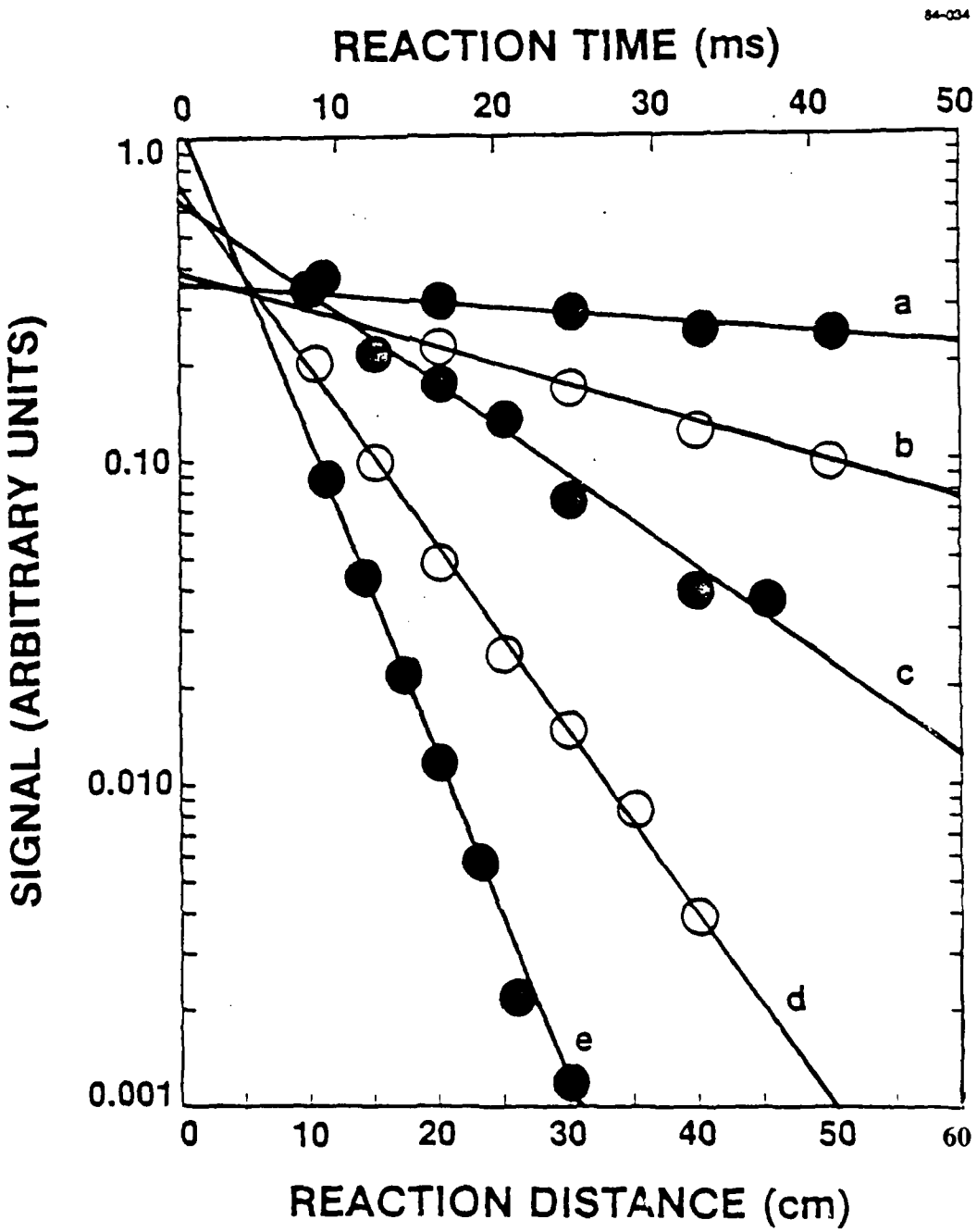

84-034
REACTION TIME (ms)
0
10
20
30
40
50
1.0
0.10
0.010
0.001
SIGNAL (ARBITRARY UNITS)
a
b
c
d
e
0
10
20
30
40
50
60
REACTION DISTANCE (cm)

FIGURE 2

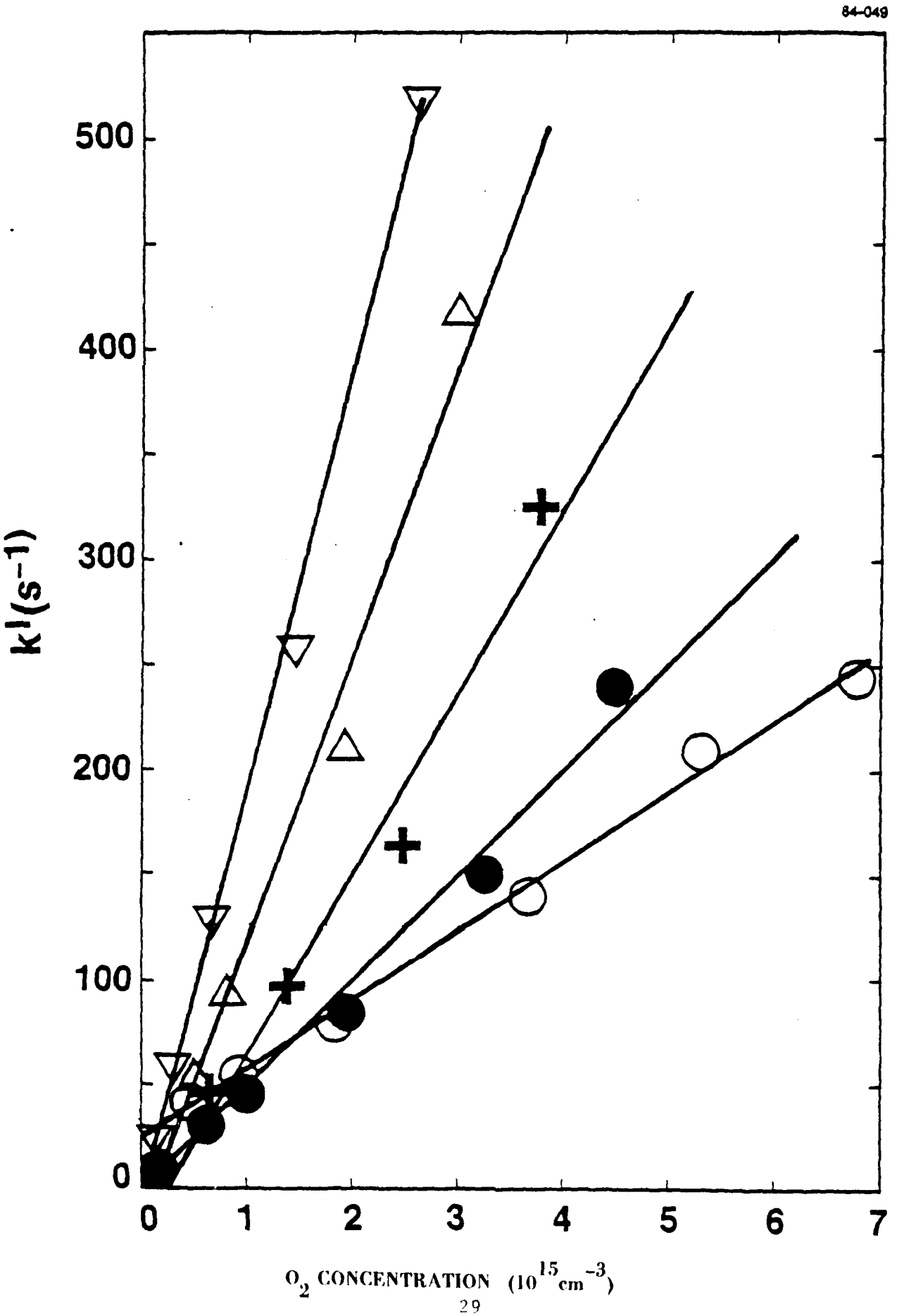

84-049
500
400
300
200
100
0
$k^1(s^{-1})$
0
1
2
3
4
5
6
7
O_2 CONCENTRATION (10^{15} cm^{-3})

FIGURE 3

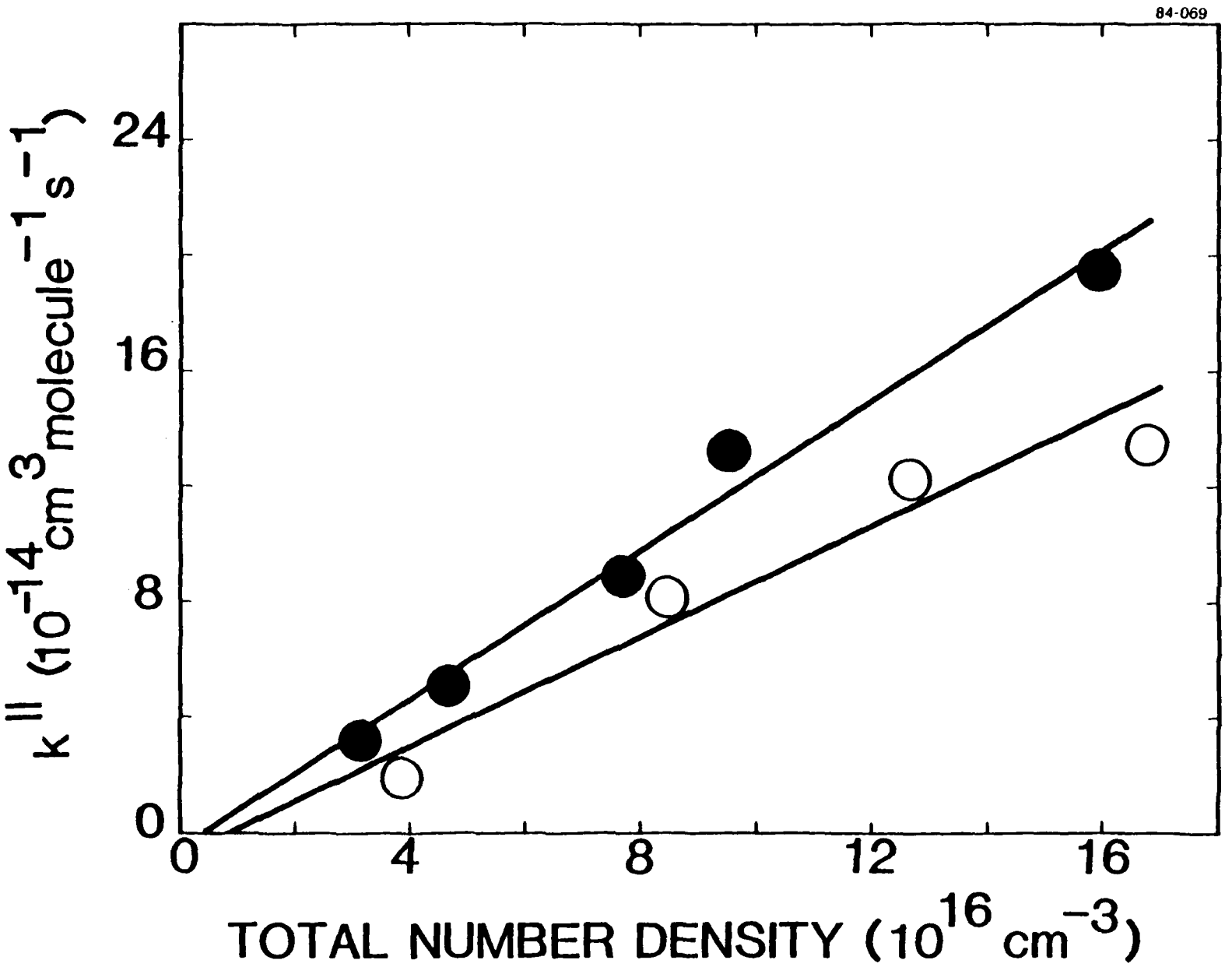

84-069
k^{II} (10^{-14} cm^3 $molecule^{-1}$ s^{-1})
24
16
8
0
0
4
8
12
16
TOTAL NUMBER DENSITY (10^{16} cm^{-3})

FIGURE 4

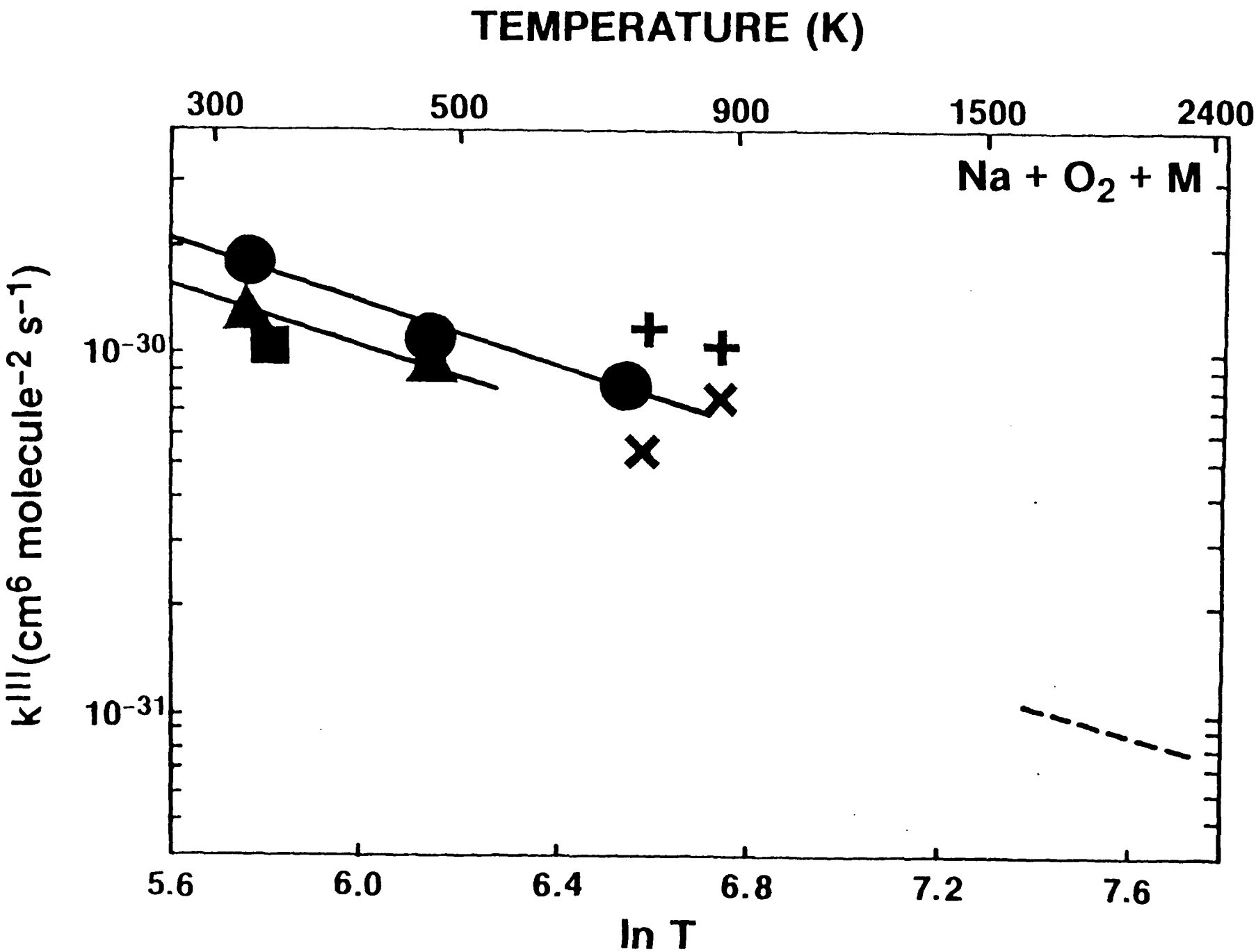

TEMPERATURE (K)
300
500
900
1500
2400
Na + O_2 + M
k^{III}(cm^6 molecule^{-2} s^{-1})
10^{-30}
10^{-31}
5.6
6.0
6.4
6.8
7.2
7.6
ln T

FIGURE 5

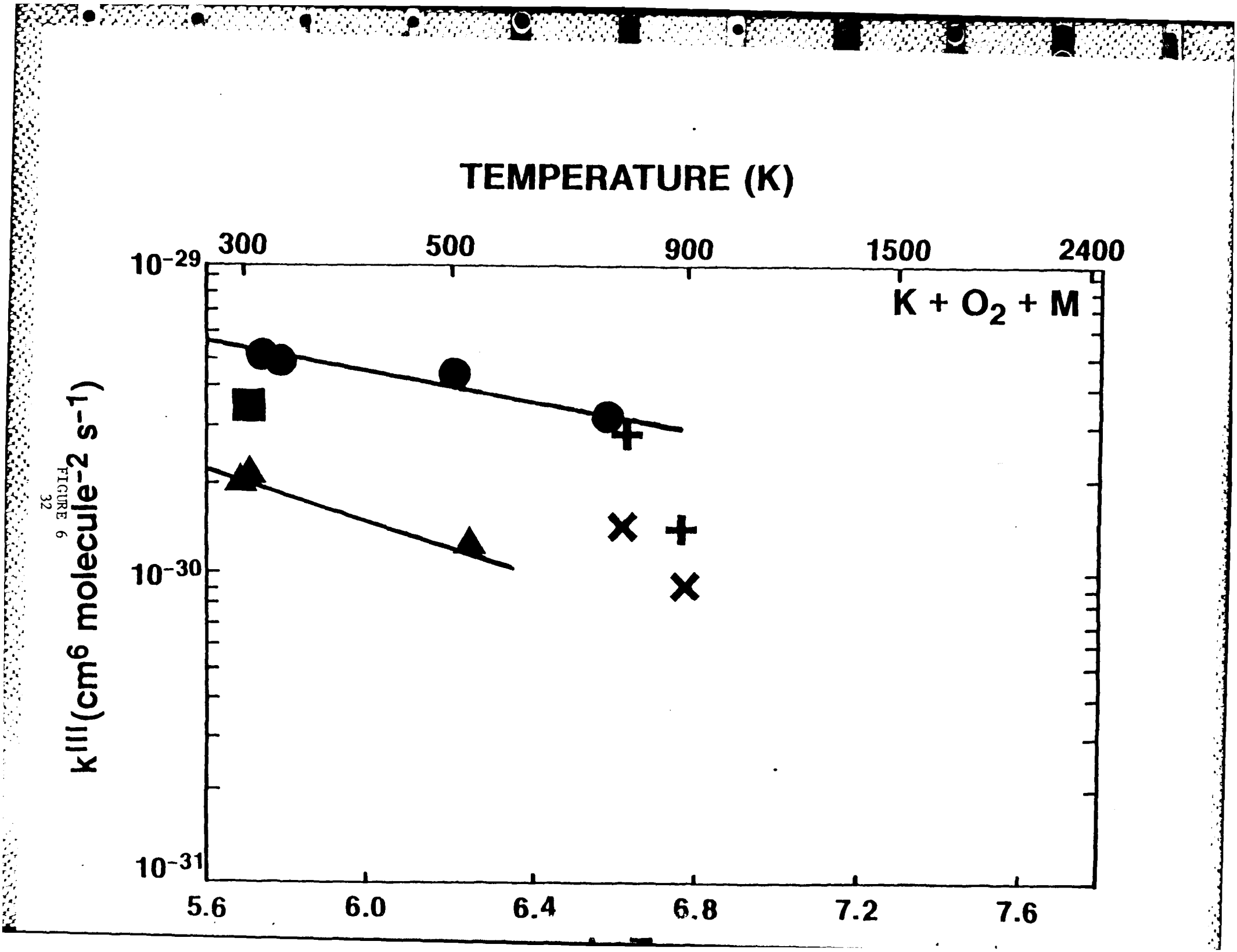

TEMPERATURE (K)
300
500
900
1500
2400
10^{-29}
10^{-30}
10^{-31}
$K + O_2 + M$
$k^{III}(cm^6\ molecule^{-2}\ s^{-1})$
5.6
6.0
6.4
6.8
7.2
7.6

FIGURE 6
32

3. THE GAS PHASE REACTION RATE OF SODIUM HYDROXIDE WITH HYDROCHLORIC ACID

(To be submitted to the Journal of Physical Chemistry.)

ABSTRACT

The reactions of metallic species introduced into the atmosphere by meteor ablation may play a significant role in stratospheric chemistry. In particular, it has been suggested that the reaction of NaOH with HCl might affect the concentration of odd chlorine, thus having an impact on the ozone balance. This paper describes the first measurement of this reaction rate constant. At 308 K, we find that $k = (2.8 \pm 0.9) \times 10^{-10}$ cm^3 molecule^{-1} s^{-1}. As a result of the methods developed to perform this measurement, we have also determined estimates of the following room temperature rate constants in units of cm^3 molecule^{-1} s^{-1}: $k(NaO + HCl \rightarrow NaCl + OH) \cong 2.8 \times 10^{-10}$, $k(NaOH + H \rightarrow Na + H_2O) > 4 \times 10^{-12}$, $k(NaCl + H \rightarrow Na + HCl) \cong 5 \times 10^{-(14 \pm 1)}$ and $k(Na + H_2O_2) \cong 6.9 \times 10^{-11}$, where approximately 0.6 of the reactions produce NaOH + OH, with the remainder forming NaO + H_2O.

INTRODUCTION

Metallic elements volatilized during meteor entry into the Earth's upper atmosphere play a significant role in the structure of the D and E regions of the ionosphere,[1-2] and, at least in the case of sodium, the visible day and nightglow emissions from the mesosphere and lower thermosphere.[3-5] Recently, it was suggested that sodium and other meteor metals may be important in stratospheric chemistry by affecting ozone reduction by the catalytic chlorine cycle.[6-8]

The influx of meteor metals into the upper atmosphere has been estimated[9] to be 3.5×10^6 kg yr^{-1}, with a sodium abundance of 2% leading to a calculated sodium flux of 1.2×10^4 atoms cm^{-2} s^{-1}. Other estimates of sodium flux run

as high as 2×10^4 cm^{-2} s^{-1}.[10] The flux of other metallic species such as Mg, Ca, Al, Si and Fe will be as much as 10 times higher and speculative concerns about their influence on upper atmospheric homogeneous and heterogeneous chemistry have been published.[1-2,7-8,10]

Unfortunately, all attempts to model the role of volatilized meteor metals (particularly sodium) in the mesosphere and stratosphere[3-4,7,9-15] have suffered from an almost total lack of measured rate constants. All such models start with the oxidation of sodium or other metallic species in reaction with atmospheric O, O_2, or O_3. However, the only measured chemical rate constants currently available for any alkali meteor metal oxidation reactions are those for the three body recombination reactions of alkali atoms (Na, K) with O_2[16-18]

$$Na \text{ or } K + O_2 + M \rightarrow NaO_2 \text{ or } KO_2 + M \quad . \qquad (1)$$

In fact, until two years ago, even this reaction was thought to be ~1000 times slower[19-20] than the value found in the more recent measurements.

From the recent modeling work[7-8,10,13,21-22] and comparison of these models with atmospheric measurements,[12,14-15] neutral sodium is believed to be transformed via a series of chemical reactions involving NaO and NaO_2 intermediates to NaOH. A survey of the relevant literature[6-8,10,13] provides a fairly complete list of possible neutral sodium reactions of importance, and a simplified schematic diagram of these reactions is shown in Figure 1.

Neutral sodium appears in a range between 110 and 70 km altitude. As shown in Figure 1, the main removal mechanisms are by reaction with O_2 or O_3, the latter used by Chapman[23] to explain the Na nightglow. We have recently completed temperature dependent measurements of the reaction rates with O_2 in our laboratory which show that this reaction proceeds with a fast three body rate constant of 1.9×10^{-30} cm^6 s^{-1} with N_2 as the third body at 300 K.[18] This, leads us to believe that most of the Na in the lower mesosphere is

converted to NaO_2, since the three body recombination rate with O_2 exceeds even a gas kinetic two body rate with O_3 below 80 km. Since none of the remaining rates have ever been measured, the rest of the mechanism (as proposed by various models) is speculative. However, the dominant sodium species which leave the mesosphere and enter the stratosphere are probably NaOH and/or NaO_2.

The fate of NaOH is very uncertain. Indeed, only in the past few years has NaOH been recognized as a major reaction product. Ferguson[6] suggested that it forms NaOH cluster ions of the form $H^+(NaOH)_n\ (H_2O)_m$, which either may be rained out from the troposphere or removed in the stratospheric aerosol layer. In a recent paper by Murad et al,[8] it was proposed that the reactions of metal hydroxides (and superoxides) with chlorine compounds between 40 and 70 km may have an impact on the depletion of stratospheric ozone. In the case of sodium, the exothermic bimolecular reactions

$$NaOH + HCl \rightarrow NaCl + H_2O \qquad \Delta H_r^o = -133 \pm 13 \text{ kJ mol}^{-1}\ , \qquad (2)$$

$$NaOH + ClO \rightarrow NaCl + HO_2 \qquad \Delta H_r^o = -63 \pm 15 \text{ kJ mol}^{-1}\ , \text{ and} \qquad (3)$$

$$NaOH + Cl \rightarrow NaCl + OH \qquad \Delta H_r^o = -67 \pm 13 \text{ kJ mol}^{-1} \qquad (4)$$

might be expected to proceed rapidly and act as a sink for Cl, given that NaCl can readily polymerize and condense via heterogeneous nucleation.[8] Murad et al calculated that if k_2 were $\sim 10^{-11}$ cm^3 $molecule^{-1}$ s^{-1}, then the reaction of NaOH with HCl would be comparable to the major recognized Cl regeneration mechanism,

$$OH + HCl \rightarrow Cl + H_2O\ . \qquad (5)$$

While previously published studies have viewed NaCl as a potential sink for stratospheric chlorine,[7-8] more recent analyses by F. Rowland[24] indicate that photolysis of NaCl may in fact release free Cl. Given the potentially large J values (photolysis rates) for this process,[24] reactions (2) - (4) could effectively supplement, rather than remove, reaction (5) as a release mechanism for Cl from the inactive HCl stratospheric reservoir and thereby determine the extent to which ozone might be depleted by chlorine compounds in the stratosphere. However, to understand fully the role of alkali species in the atmosphere, one must also consider the effects of NaO_2 and NaOH photodissociation on these processes.[13,25]

The purpose of this study is to provide a direct experimental rate measurement of the reaction NaOH + HCl → NaCl + H_2O, which serves as a starting point for understanding the stratospheric role of sodium and other meteor metals. Only by obtaining accurate, directly measured rate constants can we hope to understand atmospheric metal chemistry, and in particular, how this chemistry affects the ozone balance.

EXPERIMENTAL

Very little gas phase research has been done on alkali hydroxides because they are difficult to vaporize,[26] are extremely corrosive,[27] and readily dimerize in the gas phase.[28] In addition, there are no established detection techniques sensitive enough to make kinetic analyses of alkali hydroxide reactions. With this in mind we have taken an indirect approach for producing and detecting NaOH, i.e., chemical production of NaOH by the reaction of atomic sodium with hydrogen peroxide, and detection of NaOH by chemical conversion back to atomic sodium, which is then observed using laser induced fluorescence.

The measurements were performed in the Aerodyne high temperature fast flow reactor, which is fully described in Reference 29 and whose relevant features are illustrated in Figure 2. Briefly, a 7.26 cm diameter, 120 cm long alumina tube is used, fitted with Kanthal heater elements which can

radiatively heat the tube over the temperature range 294 K - 1500 K. Four perpendicular alumina side arms at the tube exit permit detection of flow species by a variety of optical techniques, including laser- or resonance lamp-excited fluorescence, infrared absorption (either broadband or high resolution), and observation of chemiluminescence. Gas temperatures are obtained with chromel-alumel or shielded W-5%Re/W-26%Re thermocouples.[30] Extensive calibrations indicate the temperature can be measured with an accuracy of ±10 K over the entire operating range of the reactor for flow Reynolds numbers below 500; for the current experiment R_e is typically below 50. The gas is pumped by a Kinney KMBD 1602 mechanical pump and Roots blower with an effective pumping speed of 450 liters s^{-1}. The helium carrier gas is added at the entrance of the flow tube through mullite multichannel arrays which laminarize the flow. These are ~2.5 cm upstream of the outlet of the reactant inlet tube and 78 cm from the detection region. This allows sufficient distance (18 cm) for the helium flow to mix with the reactants and develop a parabolic velocity profile before reaching the reaction zone. Gas volumetric flow rates are determined using calibrated thermal conductivity type mass flow meters. Flow speeds can be varied from 4 to 100 m s^{-1}. A calibrated MKS Baratron Model 310-BSH10 capacitance manometer (0.8% accuracy) is used to measure pressure.

Alkali atoms are generated by heating the sample in a 2.5 cm dia cylindrical monel oven to a temperature commensurate with attaining a vapor pressure of that species of 10^{-6} to 10^{-4} torr within the oven. The oven is silver plated to resist alkali corrosion.[27] The vapor is entrained in a flow of inert carrier gas and introduced into the flow tube through a 10 cm section of 19 mm o.d. silver tubing. The sodium vapor is further diluted by the carrier gas in the main flow tube so that the sodium concentration within the reaction zone is always less than 10^{10} cm^{-3}. For wall removal rate measurements the entire oven assembly may be placed downstream of the mullite arrays as a movable source. Since the oven is heated, it warms the main carrier gas flow slightly. Axial temperature surveys in the reaction region show that the final flow temperature profile is uniform at a value of 308 K.

Sodium hydroxide is produced via the reaction

$$Na + H_2O_2 \rightarrow NaOH + OH \qquad \Delta H_r^o = -130 \pm 13 \text{ kJ mol}^{-1} \qquad (6)$$

The H_2O_2 is added upstream of the mullite arrays with the main carrier gas. An all glass and teflon inlet system is used to prevent decomposition of H_2O_2 between its reservoir and the flow tube. Flow rates of H_2O_2 are determined by entraining the vapor in a measured helium flow at a known total reservoir pressure, where

$$\text{Flow } H_2O_2 = \left(\frac{P_{H_2O_2}}{P_{total}}\right) \times (\text{flow helium through system}) \qquad (7)$$

The partial pressure of H_2O_2 at 25°C is 2.0 torr.

Detection of NaOH is accomplished by converting it back to atomic sodium in the detection region, where the sodium is measured by laser induced fluorescence (LIF). This conversion is accomplished by injecting an excess of atomic hydrogen into the flow 2 cm upstream of the LIF detector.

$$NaOH + H \rightarrow Na + H_2O \qquad \Delta H_r^o = -154 \pm 13 \text{ kJ mol}^{-1} \qquad (8)$$

$$Na + h\nu \rightarrow Na^* \rightarrow Na + h\nu \qquad \text{LIF Detection} \qquad (9)$$

The hydrogen atoms, produced by microwave discharge of pure molecular hydrogen, are introduced through a teflon-lined 6 mm dia. tube. With the mean flow velocity of 1000 cm s^{-1}, the reaction time of hydrogen in the detector (t_d) is 2 ms. The atomic hydrogen concentration is estimated to be 2×10^{14} cm^{-3}, by measuring the H_2 flow rate and assuming that 10% of the H_2 passing through the discharge dissociates,[31] with no recombination[32] or loss on the inlet tube walls.[31]

A Molectron DL14 nitrogen pumped dye laser is used for laser induced fluorescence detection of Na. The laser induced fluorescence data acquisition system, and manipulation of data have been detailed elsewhere.[33] However, it should be noted that fluorescence is usually averaged over 100 laser pulses, accounting for nonfluorescent background signals and for pulse-to- pulse fluctuations in laser intensity. The combined signal-to-noise ratio for these measurements generally exceeds 25.

Purities of the chemicals used in these experiments are as follows: sodium metal, 99.95% (Alfa); helium, 99.995% (Northeast Cryogenics); hydrogen, 99.995% (Air Products); nitrogen, 99.998% (Northeast Cryogenics); and hydrogen chloride, 99.99% (Northeast Cryogenics). Hydrogen peroxide, obtained as a 90% (by weight) solution from FMC Corporation, is purified by vacuum distillation. Titration with potassium permanganate indicates a resulting purity on the order of 99%. This corresponds to a purity in the vapor phase of ~93%, with the balance being water vapor.

Rate measurements are made using one reactant in excess of the other (detected) reactant, thus ensuring pseudo-first order kinetic conditions. Reaction times are varied by changing the injector position at fixed total flow velocity and pressure. Corrections for both axial and radial diffusion and wall removal are made using the procedure outlined by Brown.[34] This method is based on a numerical solution of the equations describing diffusion and reaction in a flow tube. It assumes that Poiseuille flow exists and provides ranges for k, k_w (wall removal), and D (diffusion coefficient) for which the solutions have been shown to be valid. Wall removal rates of the measured species are determined in separate experiments by varying the oven position. The observed wall removal rate, as well as the reaction rate, is corrected for diffusion effects. Diffusion constants for alkali atoms and hydroxides were obtained from wall removal measurements in the instance where the observed disappearance of the species is diffusion limited.[35] At 308 K, D(Na-He) = 0.53 atm cm^2 s^{-1}, and D(NaOH-He) = 0.47 atm cm^2 s^{-1}.

An important aspect of the data analysis is the ability to ensure that secondary reactions have no effect on the concentration of the species being monitored. This could dramatically affect the accuracy of the rate measurements. The effects of secondary reactions are determined by modeling the reactions occurring in the flow tube. This is done using the Aerodyne PACKAGE code,[36] a kinetic modeling program which numerically integrates the differential rate equations for a specified set of reactions. Backward reaction rates determined from the JANAF thermochemical tables and the forward rates are included, to ensure that accuracy is maintained.

RESULTS

Na + H_2O_2 Reaction

The NaOH formation rate was measured by directly observing the disappearance of sodium, with H_2O_2 in known excess. The reaction has two exothermic product channels,

$$Na + H_2O_2 \rightarrow NaOH + OH \qquad \Delta H_r^o = -130 \pm 13 \text{ kJ mol}^{-1} \qquad (6)$$

$$\rightarrow NaO + H_2O \qquad \Delta H_r^o = -130 \pm 42 \text{ kJ mol}^{-1} \qquad (6')$$

so what is measured by monitoring Na disappearance is the total reaction rate. However, one can add excess CO (~2×10^{15} cm^{-3}), which rapidly and quantitatively converts NaO to Na,[37-38]

$$NaO + CO \rightarrow Na(^2S) + CO_2 \qquad \Delta H_r^o = -259 \pm 42 \text{ kJ mol}^{-1} \qquad (10)$$

$$\rightarrow Na(^2P) + CO_2 \qquad \Delta H_r^o = -56 \pm 42 \text{ kJ mol}^{-1} \qquad (10')$$

Although the value for k_{10} has not been measured, indirect estimates from Reference (37) imply $k_{10} \geq 10^{-11}$ cm^3 $molecule^{-1}$ s^{-1}. The large amount of CO

added is required to ensure that all of the NaO cycles back to Na on a time scale much shorter than the time required for reaction (6) to occur.

A rate measurement with CO present results in the production rate for only the NaOH branch. The results of these measurements are shown in Figure 3. Experimental conditions are given in Table 1. The rate constant for both channels is $k_{6+6'} = (6.9 \pm 3.0) \times 10^{-11}$ cm^3 molecule^{-1} s^{-1}, and the fraction in the NaOH product channel is 0.61 ±0.10. The major uncertainty in the rate constants k_6 and $k_{6'}$ is the H_2O_2 concentration, which is not directly measured, but is obtained as indicated earlier.

An independent determination of the product branching ratio for reaction (6) is obtained by observing the hydroxyl radical via laser induced fluorescence at 308.6 nm. When Na reacts with H_2O_2, only the NaOH product channel produces OH. However, when excess HCl is added to the NaO and NaOH product mixture, additional OH, is formed by the reaction

$$NaO + HCl \rightarrow NaCl + OH \qquad \Delta H^o_r = -134 \pm 42 \text{ kJ mol}^{-1} \qquad (11)$$

Thus a measurement of the amounts of OH produced before and after addition of HCl provides the relative amounts of NaOH and NaO originally formed from Na + H_2O_2. The observed NaOH product fraction by this method is 0.60 ±0.10, in excellent agreement with the value obtained from the rate measurements.

NaOH + HCl Reaction

In the presence of excess CO, the reaction of sodium with hydrogen peroxide produces only NaOH. Using this reaction as a source for NaOH, a series of rate measurements were made for the reaction of NaOH with HCl. First-order decays were linear for more than a factor of 10 in fluorescence signal, with the HCl concentrations ranging from 1 to 4 x 10^{12} cm^{-3}. The results of these experiments are shown in Figure 4, and the rate constant for this reaction is $k_2 = (2.8 \pm 0.9) \times 10^{-10}$ cm^3 molecule^{-1} s^{-1}. The uncertainty

expressed includes estimated precision errors at a 95% confidence level, as well as estimated errors in accuracy.

Separate measurements were also made without adding CO. In this case NaO, in addition to NaOH, is present and reacts with HCl (reaction 11), complicating the analysis. Furthermore, the detection scheme, based on conversion to Na by addition of atomic hydrogen, would not appear to distinguish between NaO and NaOH, since Na atoms are also produced in the reaction

$$NaO + H \rightarrow Na + OH \qquad \Delta H_r^o = -155 \pm 42 \text{ kJ mol}^{-1} \qquad (12)$$

Thus, without CO, the decrease in signal upon addition of HCl provides the average of reactions (2) and (11), weighted by the branching ratio from reaction (6,6'). The results, however, show the same decay with and without added CO (see Figure 4), implying that both NaO and NaOH react with HCl at approximately the same rate. This observation is reasonable if one considers the hydroxyl group on NaOH to act as a quasi-atom in respect to its chemical behavior given identical exothermicities for both reactions.

Separate OH measurements confirm that atomic hydrogen reacts with NaO as well as with pure NaOH. Although we could not measure the NaO + HCl rate constant directly, the observation that 1) OH is formed in the NaO + H reaction (proving the existence of NaO), 2) OH is also formed upon addition of HCl to NaO, and 3) the decay rates with added HCl are identical both with or without CO, imply that NaO reacts with HCl at approximately the same rate as NaOH.

Detector Corrections and Modeling

Although the plots of ln (signal) vs. reaction time are linear over the first order of magnitude decrease in signal, at longer times they flatten out at a value typically a few percent of the initial (zero reaction time) signal

(Figure 5). This effect can be attributed to an additional component to the Na signal from the reaction

$$NaCl + H \rightarrow Na + HCl \qquad \Delta H_r = -21 \pm 2 \text{ kJ mol}^{-1} \tag{13}$$

For the case with CO present, sodium formed in the detection region by addition of atomic hydrogen has two sources, NaOH and NaCl, the amount of each depending on the extent to which the $NaOH + HCl \rightarrow NaCl + H_2O$ reaction has gone to completion. The rate equation for the formation of sodium in the detector is

$$\frac{d[Na]}{dt} = k_8 [NaOH]_d [H] + k_{13} [NaCl]_d [H] \tag{14}$$

where the d subscript indicates the concentration at the entrance to the detector zone. Integrating over the detector reaction time (t_d), assuming excess hydrogen, we obtain

$$[Na] = [NaOH]_d (1 - e^{-k_8 [H] t_d}) + [NaCl]_d (1 - e^{-k_{13} [H] t_d}) \tag{15}$$

If no HCl is added, the observed LIF signal arises solely from NaOH. We have observed that this signal (after correcting differences in diffusion and wall removal between Na and NaOH) is identical to that arising from only sodium (i.e., without H_2O_2 added). This means that within the available detector reaction time, all of the NaOH is converted to sodium, with an estimated error of 20%. This sets a lower limit to $k_8 [H] t_d$. Given t_d = 2 ms and $[H] \approx 2 \times 10^{14}$ cm^3, this requires that $k_8 \geq 4 \times 10^{-12}$ cm^3 molecule^{-1} s^{-1}. The accuracy of t_d is ±0.5 ms. If less than 10% of the H_2 is dissociated (it is unlikely to be higher under our operating conditions), then k_8 is faster than the stated limit.

This value for k_8 is in reasonable agreement with a value of $1 \times 10^{-12}\ T^{1/2}$ (1.7×10^{-11} cm^3 molecule^{-1} s^{-1} at 300 K) which is used by Hynes, et al.[17] in fitting their flame data over a wide range of conditions, and also with $2 \times 10^{-11}\ e^{-800/T}$ (1.4×10^{-12} at 300 K), which is used in various atmospheric models.[10,13] The former value is claimed to be accurate to within a factor of two at flame temperatures, and the latter is only an estimate. We are planning to perform direct measurements of this reaction in the near future.

Now if we measure the reaction rate of NaOH + HCl, at short reaction times the decay in signal is logarithmic because $[NaOH]_d > [NaCl]_d$, and only the first term in Eq. (15) is significant. At long reaction times, $[NaCl]_d > [NaOH]_d$ and the second term becomes dominant (Figure 5). If $k_{13} = k_8$, we would never observe a decay in [Na] since both terms in Eq. (15) would always have the same sum. However, the fact that an initial decay is observed with a later leveling of signal shows that $k_{13} << k_8$ and, from the relative value of the signal where it levels off, we can estimate k_{13}.

To determine k_{13}, we modeled this reaction system using the conditions in Table 2 and rate set in Table 3. This rate set is more extensive than the above discussion implies because there could be secondary reactions between the excess H_2O_2 and the sodium formed in the detector, as well as other minor OH, H, etc. reactions. This model also includes the undissociated hydrogen, and the water impurity (~7%) in the H_2O_2. We systematically varied k_8, k_{13}, [H], $[H_2O_2]$, and t_d. The results show that all secondary reactions have little effect (< 5%) on the calculated sodium densities, and that the variations of Na with $[H_2O_2]$ and $[H_2]$ are small, in reasonable agreement with additional experiments. The value for k_{13} which best fits the experimental data is $(8 \pm 3)/[H]$, which leads to value of k_{13} in the range 1×10^{-14} to 5×10^{-13} cm^3 molecule^{-1} s^{-1}, with a best estimate of 5×10^{-14} cm^3 molecule^{-1} s^{-1}. In light of the small exothermicity for this reaction, this value is not unreasonable. If the rate constant is expressed in the Arrhenius form, $k = Ae^{-E/RT}$, this would correspond to only a 21 kJ mol^{-1} barrier, even with a gas kinetic pre-exponential term.

DISCUSSION

The reaction rate constant of HCl with NaOH is found to be in its gas kinetic limit. Given the large exothermicity, absence of obvious steric effects, and the fact that reactant and product states correlate on a singlet potential energy surface, one might not consider this surprising. On the other hand, the strong covalent HCl bond must be broken during the reaction with an efficiency approaching unity. One can calculate a rate constant for this reaction using simple close collision theory.[43] This procedure assumes that the attractive portion of the intermolecular potential varies as Cr^{-6}, where C depends on the dipole moments and static polarizabilities of the reactants,[44] and r is the intermolecular distance. The total effective potential energy curve at large r is this attractive portion plus a centrifugal term which accounts for orbital angular momentum. The rate of close collisions is identified as applying to collisions with total energy sufficient to surmount the orbital angular momentum barrier in this effective potential energy curve. If it is assumed that all close collisions react, and that there is no activation energy, the rate constant calculated for NaOH + HCl is 1.8×10^{-10} cm^3 $molecule^{-1}$ s^{-1}, in good agreement with the measured value.

Few gas phase reactions of alkali molecules have been studied, none involving alkali hydroxides. The alkali-hydroxide bond is ionic in character, so that $(OH)^-$ is a closed shell species, not dissimilar to its isoelectronic and isobaric analog, F^-. Thus, in absence of data on NaOH, we can use available information on NaF and other alkali halides to try to understand the properties of the alkali hydroxides. There have been a number of molecular beam scattering measurements of alkali halides with other alkali halides or hydrogen halide molecules.[45] As a class, they all imply the existence of a strong collision complex. In the case of CsCl + KI → CsI + KCl, the reaction proceeds without any activation energy (despite being four-centered) and has a large total cross section.[46] This has been explained by the large ionic character of both species, and by the fact that alkali halide dimers have large binding energies in the geometry of a cyclic planar rhomboid.[45] This

ion-pair intermediate formulation has also been invoked in describing the BaI_2 + HCl reaction,[47] where for large alkaline earths such as barium, we can treat BaI_2 as $(BaI)^+I^-$. What we can draw from these comparative systems is that a gas kinetic rate constant, without any activation barrier is a reasonable expectation for this system. In the extrapolation of the measured rate data to lower temperatures characteristic of the stratosphere, one would not expect any great dependence on temperature for the reaction rate.

The importance of reaction (2) in stratospheric ozone chemistry may be estimated by comparing the Cl regeneration rates from HCl via reaction with OH, versus reaction with NaOH followed by photolysis of NaCl. Estimates of stratospheric NaCl photolysis rates by Rowland and Rogers[24] are in the range from 10^{-2} to 10^{-3} s^{-1}. At 40 km, the meteoric sodium is partitioned among the species NaOH, NaO_2 and NaO. Estimates of total stratospheric sodium concentrations by Liu and Reed[10] are on the order of 5×10^5 cm^{-3}. If all of the meteoric sodium were in the form of NaOH at 40 km, our measurement of k_2 would give a first order rate constant for Cl formation of 1.4×10^{-4} s^{-1}, providing that J_{NaCl} is in the range estimated by Rowland and Rogers. This is a factor of ~ 20 faster than the first order rate constant for Cl regeneration from OH + HCl of 6×10^{-6} s^{-1}, based on an OH concentration of 10^7 cm^{-3} and the value $k_5(250\ K) = 5.7 \times 10^{-13}$ cm^3 $molecule^{-1}$ s^{-1}.[48] Although the partitioning of total sodium among NaOH, NaO, and NaO_2 requires a more detailed knowledge of rate constants for the processes shown in Figure 1, this calculation demonstrates that even if only 5% is in the form of NaOH, regeneration of Cl from HCl via alkali chemistry would be comparable to regeneration by the OH reaction.

This simple computation leads us to two conclusions. First, our results for this and the other alkali reactions described show that meteoric metal reactions may have a potentially significant impact on our understanding of chemistry in the mesosphere and upper stratosphere. The large values of the sodium rate constants measured in this study emphasize this possibility. Secondly, it clearly motivates the need for further investigation of this chemistry, via detailed models, additional laboratory measurements of reaction

rate constants and photolysis cross sections, and direct measurement of molecular sodium concentration profiles in the upper atmosphere.

ACKNOWLEDGEMENTS

The authors would like to thank Drs. F. Kaufman, M. McElroy, and E. Murad for their helpful discussions and insights, and W. Goodwin for his excellent technical assistance. This work was supported by the Chemical Manufacturers Association under Contract Number FC82-401, by the Air Force Geophysics Laboratory under Contract Number F19628-83-C-0010, and by the Army Research Office under Contract Number DAAG29-81-C-0024.

REFERENCES

1. E. Murad, J. Geophys. Res., 83, 5525 (1978).

2. T.L. Brown, Chem. Rev., 73, 645 (1973).

3. J.E. Blamont, and T.M. Donahue, J. Geophys. Res., 69, 4093 (1964).

4. D.M. Hunten, Space Sci. Rev., 6, 493 (1967).

5. a) V.W.J.H. Kirchhoff, B.R. Clemesha, and D.M. Simonich, J. Geophys. Res., 84, 1323 (1979);
   b) D.R. Bates, and P.C. Ojha, Nature, 286, 790 (1980).

6. E.E. Ferguson, Geophys. Res. Lett. 5, 1035 (1978).

7. E. Murad, and W. Swider, Geophys. Res. Lett., 6, 929 (1979).

8. E. Murad, W. Swider, and S.W. Benson, Nature, 289, 273 (1981).

9. E.S. Richter, and C.F. Sechrist, Jr., J. Atmos. and Terres. Phys., 41, 579 (1979); Geophys. Res. Lett., 6, 183 (1979).

10. S.C. Liu, and G.C. Reid, Geophys. Res. Lett., 6, 283 (1979).

11. a) W.J. Baggaley, Nature, 257, 567 (1975);
    b) W.J. Baggaley, Nature, 267, 376 (1977);
    c) M.A. Hapgood, Nature, 286, 582 (1980).

12. V.W.J.H. Kirchhoff, B.R. Clemesha, and D.M. Simonich, J. Geophys. Res., 86, 6892 (1981).

13. N.D. Sze, M.K.W. Ko, W. Swider, and E. Murad, Geophys. Res. Lett., 9, 1187 (1982).

14. V.W.J.H. Kirchhoff, Geophys. Res. Lett., 10, 721 (1983).

15. L. Thomas, M.C. Isherwood, and M.R. Bowman, J. Atm. Terrestrial Phys., 45, 587 (1983).

16. D. Husain, and J.M.C. Plane, J. Chem. Soc. Far. Trans. 2, 78, 163 (1982).

17. A.J. Hynes, M. Steinberg, and K. Schofield, Submitted for publication in J. Chem. Phys.

18. J.A. Silver, M.S. Zahniser, A.C. Stanton, and C.E. Kolb, "Temperature Dependent Termolecular Reaction Rate Constants for Potassium and Sodium Superoxide Formation", submitted for publication.

19. R. Carabetta, and W.E. Kaskan, J. Phys. Chem., 72, 2483 (1968).

20. M.J. McEwan, and L.F. Phillips, Trans. Faraday Soc., 62, 717 (1966).

21. C.E. Kolb, and J.B. Elgin, Nature, 263, 488 (1976).

22. D.M. Simonich, B.R. Clemesha, and V.W.J.H. Kirchoff, J. Geophys. Res., 84, 1543 (1979).

23. S. Chapman, Astrophys. J., 90, 309 (1939).

24. F.S. Rowland, and P.J. Rogers, Proc. Natl. Acad. Sci. USA, 79 (1982).

25. F.S. Rowland, and Y. Makide, Geophys. Res. Lett., 9, 473 (1982).

26. JANAF Thermochemical Tables, The Dow Chemical Company, Midland, Michigan (1970).

27. N. Acquista, and S. Abramowitz, J. Chem. Phys., 51, 2911 (1969).

28. R.C. Schoonmaker, and R.F. Porter, J. Chem. Phys., 28, 454 (1958).

29. M.E. Gersh, J.A. Silver, M.S. Zahniser, C.E. Kolb, R.G. Brown, C.M. Gozewski, S. Kallelis, and J.C. Wormhoudt, Rev. Sci. Inst., 52, 1213 (1981).

30. A. Fontijn, and W. Felder, J. Phys. Chem., 83, 24 (1979).

31. W.E. Jones, S.D. MacKnight, and L. Teng, Chem. Rev., 73, 407 (1973).

32. D.W. Trainor, D.O. Ham, and F. Kaufman, J. Chem. Phys., 58, 4599 (1973).
33. J.A. Silver, and C.E. Kolb, J. Phys. Chem., 86, 3240 (1982).

34. R.L. Brown, J. Res. NBS, 83, 1 (1978).

35. J.A. Silver, "Diffusion Coefficients for Gaseous Alkali Species In Helium and Nitrogen". (Manuscript in preparation).

36. V. Yousefian, M.H. Weinberg, and R. Haimes, "PACKAGE: A Computer Program for Calculation of Partial Chemical Equilibrium/Partial Finite Chemical Rate Controlled Composition of Multiphased Mixtures Under One Dimensional Steady Flow," Aerodyne Research, Inc., Report No. ARI-RR-177 (February 1980).

37. C.P. Fenimore, and J.R. Kelso, J. Am. Chem. Soc., 72, 5045 (1950).

38. R.C. Benson, C.B. Bargeron, and R.E. Walker, Chem. Phys. Lett., 35, 161 (1975).

39. D.L. Baulch, R.A. Cox, R.F. Hampson, Jr., J.A. Kerr, J. Troe, and R.T. Watson, J. Phys. Chem. Ref. Data, 9, 295 (1980).

40. R.F. Hampson, U.S. Dept. of Transportation, Report No. FAA-EE-80-17 (1980).

41. J.A. Miller, J. Chem. Phys. 74, 120 (1980).

42. D.E. Jensen, and G.A. Jones, Comb. Flame, 32, 1 (1978).

43. H.S. Johnston, "Gas Phase Reaction Rate Theory", Ronald Press, New York, 1966, Chapter 9.

44. J.O. Hirschfielder, C.F. Curtiss, and R.B. Bird, "Molecular Theory of Gases and Liquids", Wiley, New York, 1964.

45. R.R. Herm, in "Alkali Halide Vapors", P. Davidovits, and D.L. McFadden, Ed., Chapter 6, Academic Press, New York, 1979, and references therein.

46. W.B. Miller, S.A. Safron, and D.R. Herschbach, J. Chem. Phys., 56, 3581 (1972).

47. A. Freedman, R. Behrens, Jr., T.P. Parr, and R.R. Herm, J. Chem. Phys., 65, 4739 (1976).

48. M.S. Zahniser, F. Kaufman, and J. Anderson, Chem. Phys. Lett., 27, 507 (1974).

FIGURE CAPTIONS

1. Schematic diagram of atmospheric sodium chemistry

2. Schematic view of the flow tube

3. Pseudo-first order decays for Na + H_2O_2 reaction. Solid line is total reaction rate; dashed line is rate for branching to NaOH only (CO added).

4. First order reaction rates vs. [HCl] for the reactions of NaOH (NaO) + HCl. (o) without CO added; (▽) with CO added.

5. Typical decay of fluorescence signal vs. reaction time for NaOH + HCl, showing contribution to total detected sodium (___) from NaOH (---) and NaCl (••••). Circles are experimental data.

Table 1 - Typical Experimental Conditions

Temperature, K	308
Flow Velocity, m s^{-1}	10.0
Pressure, torr	2.0
[Na], cm^{-3} (initial)	$\leq 10^{10}$
[H_2O_2], cm^{-3}	1.3×10^{13}
[HCl], cm^{-3}	$1 - 4 \times 10^{12}$
[H], cm^{-3}	2×10^{14}

Table 2 - Initial Conditions Used in Chemical Model

Temperature, K	308
Flow Velocity, m s^{-1}	10.0
Pressure, torr	2.0
[Na], cm^{-3} (initial)	10^{10}
$[H_2O_2]$, cm^{-3}	1.3×10^{13}
[HCl], cm^{-3}	1.93×10^{12}
$[H]_d$, cm^{-3}	$2 \times 10^{13} - 1 \times 10^{15}$
$[H_2]_d$, cm^{-3}	$10^{15} - 10^{16}$
$[H_2O]$, cm^{-3}	7×10^{11}
t_{rxn}, ms	0 - 25
t_d, ms	0.5 - 4.0

Table 3 - Reaction Rate Set Used for Modeling Na Chemistry[a]

Reaction	k (cm^3 $molecule^{-1}$ s^{-1})	Reference
$Na + H_2O_2 \rightarrow NaOH + OH$	6.9 (-11)	This Work
$NaOH + HCl \rightarrow NaCl + H_2O$	2.8 (-10)	This Work
$NaOH + H \rightarrow Na + H_2O$	1.0 (-10) - 1.0 (-14)	This Work
$NaCl + H \rightarrow Na + HCl$	1.0 (-10) - 1.0 (-14)	This Work
$Na + HO_2 \rightarrow NaOH + O$	1.0 (-10)	Estimated
$2\ HO_2 \rightarrow H_2O_2 + O_2$	2.5 (-12)	39
$O + H_2O_2 \rightarrow OH + HO_2$	2.7 (-12) $e^{-2100/T}$	39
$OH + H_2O_2 \rightarrow H_2O + HO_2$	2.96 (-12) $e^{-164/T}$	39
$H + H_2O_2 \rightarrow H_2 + HO_2$	2.13 (-12) $e^{-1400/T}$	40
$H + H_2O_2 \rightarrow OH + H_2O$	2.76 (-12) $e^{-1400/T}$	40
$H_2 + OH \rightarrow H + H_2O$	1.8 (-11) $e^{-2330/T}$	39
$H + O_2 \rightarrow O + OH$	1.19 (-7) $T^{0.861}$ $e^{-8316/T}$	41
$H_2 + O \rightarrow H + OH$	3.0 (-14) $T^{1.0}$ $e^{-4479/T}$	42
$OH + HO_2 \rightarrow H_2O + O_2$	4.0 (-11)	40
$H + HO_2 \rightarrow 2OH$	3.2 (-11)	40
$H + HO_2 \rightarrow H_2 + O_2$	1.4 (-11)	40
$H + HO_2 \rightarrow H_2O + O$	9.4 (-13)	40
$O + HO_2 \rightarrow O_2 + OH$	8.0 (-11) $e^{-500/T}$	40
$2OH \rightarrow O + H_2O$	1.0 (-11) $e^{-550/T}$	40
$HCl + OH \rightarrow H_2O + Cl$	6.6 (-13)	39

a) No 3-body rates were used because the system is at low pressure.

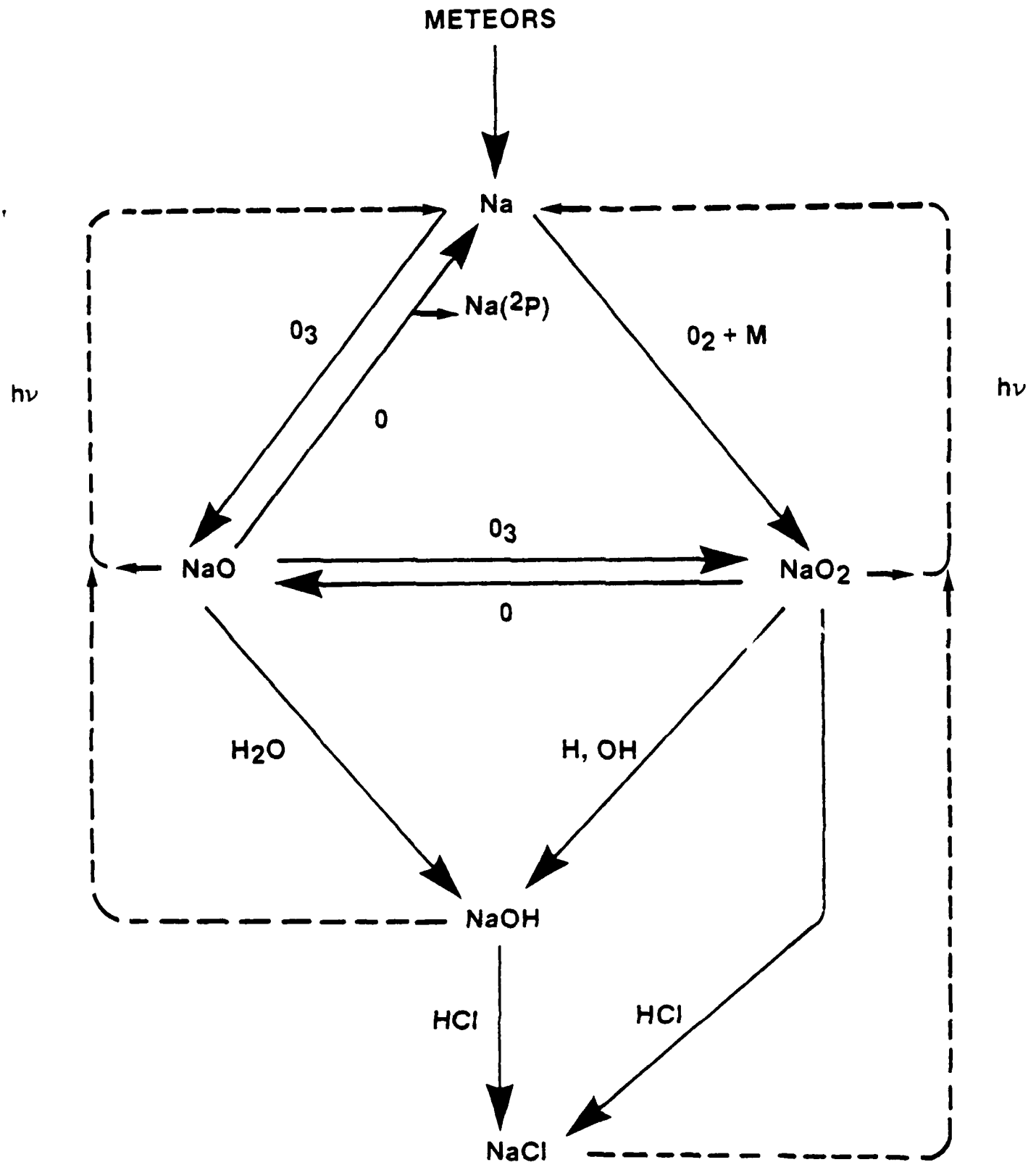

METEORS
Na
Na(2P)
O3
O2 + M
hν
hν
O
O3
NaO
NaO2
O
H2O
H, OH
NaOH
HCl
HCl
NaCl

FIGURE 1

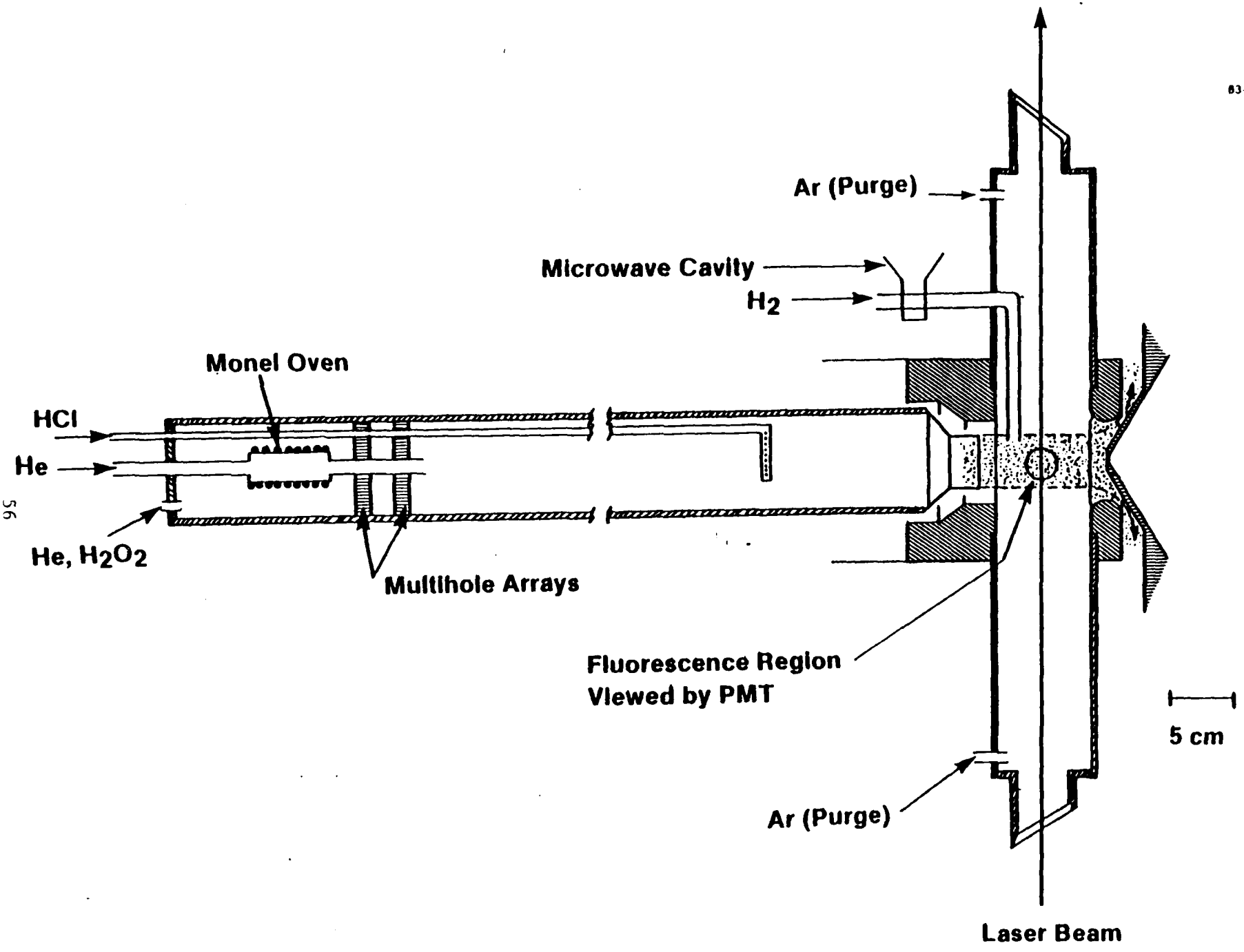

83-203
Ar (Purge)
Microwave Cavity
H_2
Monel Oven
HCl
He
He, H_2O_2
Multihole Arrays
Fluorescence Region
Viewed by PMT
5 cm
Ar (Purge)
Laser Beam

FIGURE 2

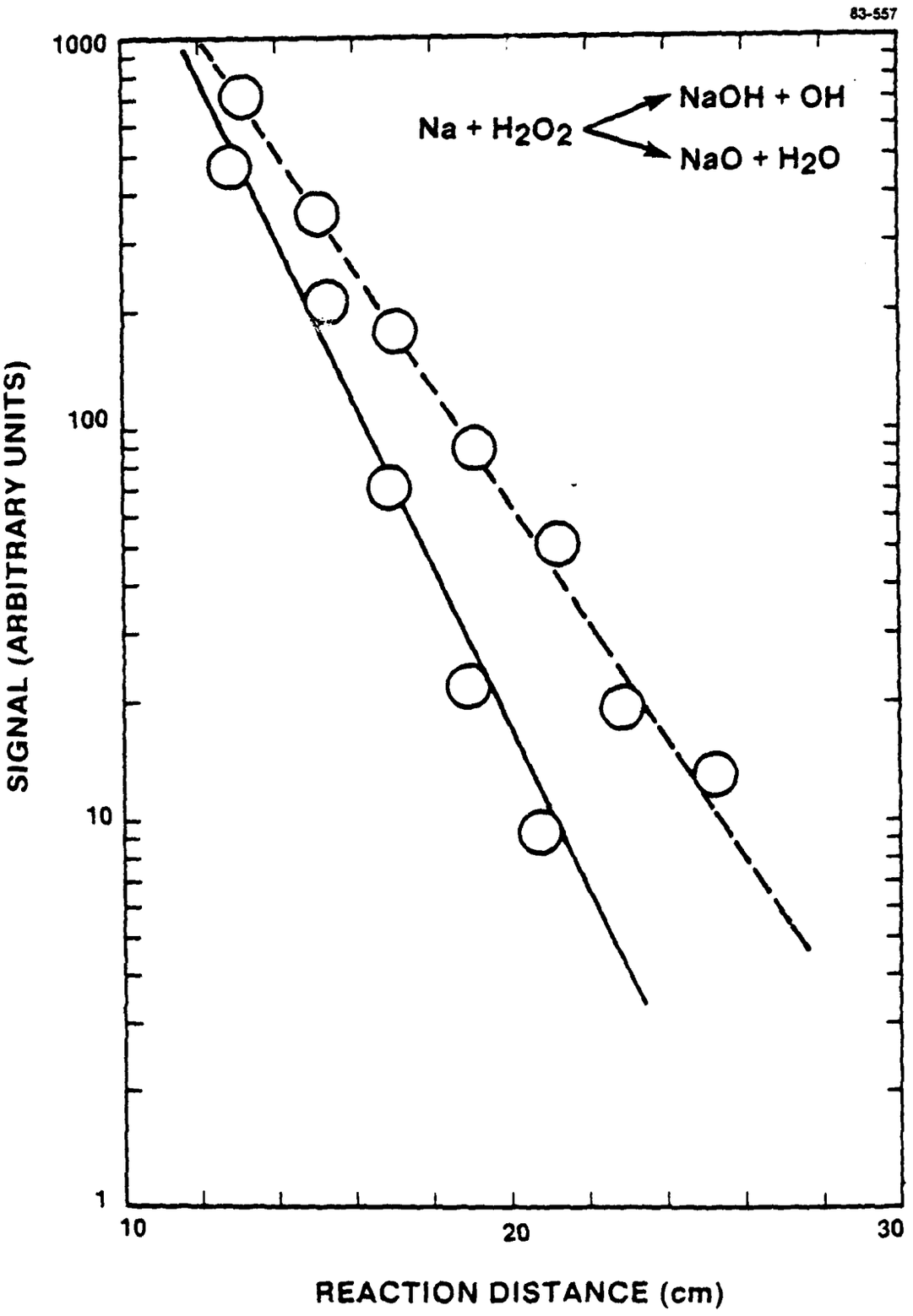

83-557
1000
100
10
1
SIGNAL (ARBITRARY UNITS)
Na + H2O2
NaOH + OH
NaO + H2O
10
20
30
REACTION DISTANCE (cm)

FIGURE 3

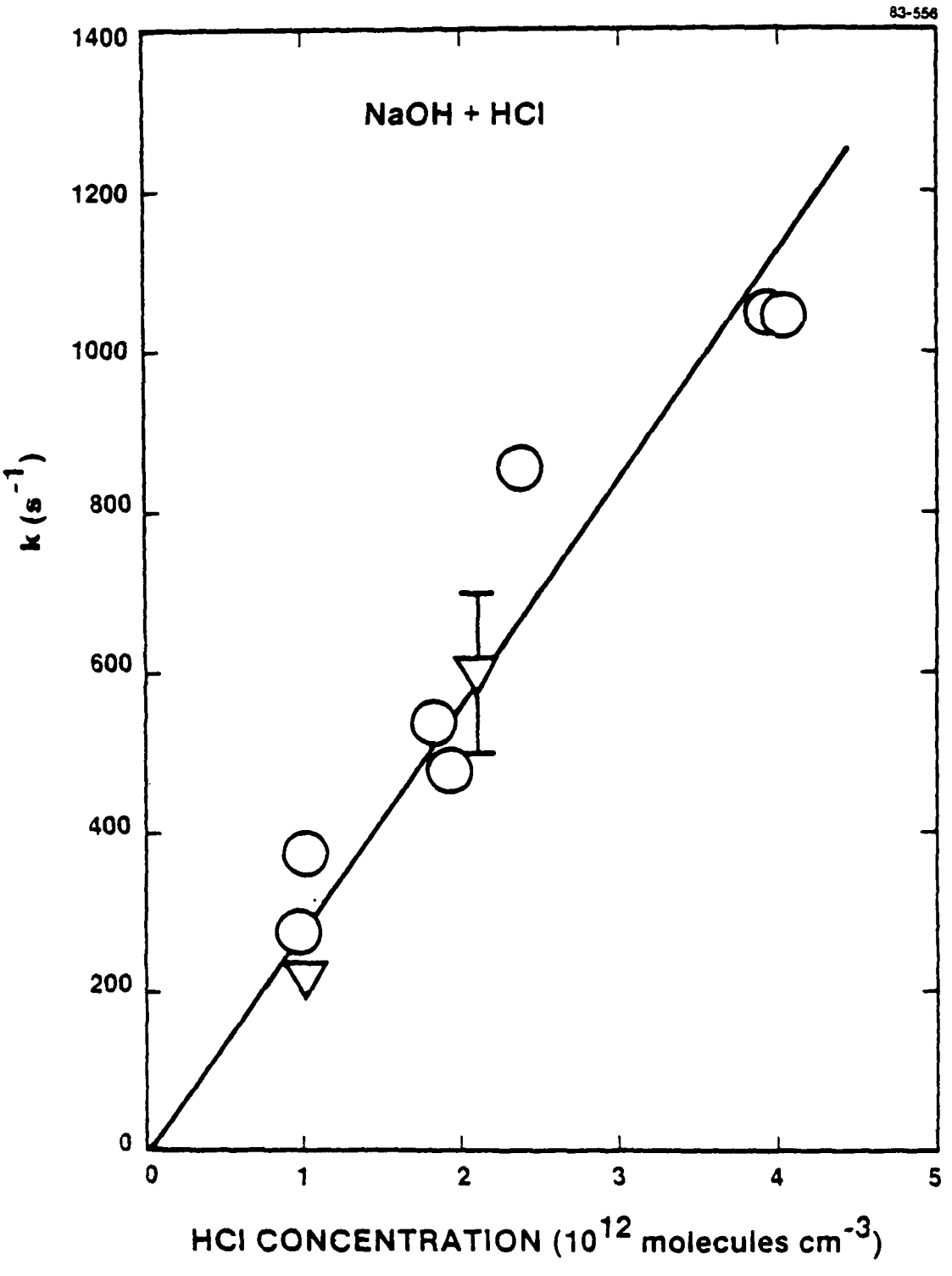

83-556
NaOH + HCl
k (s^{-1})
1400
1200
1000
800
600
400
200
0
0
1
2
3
4
5
HCl CONCENTRATION (10^{12} molecules cm^{-3})

FIGURE 4

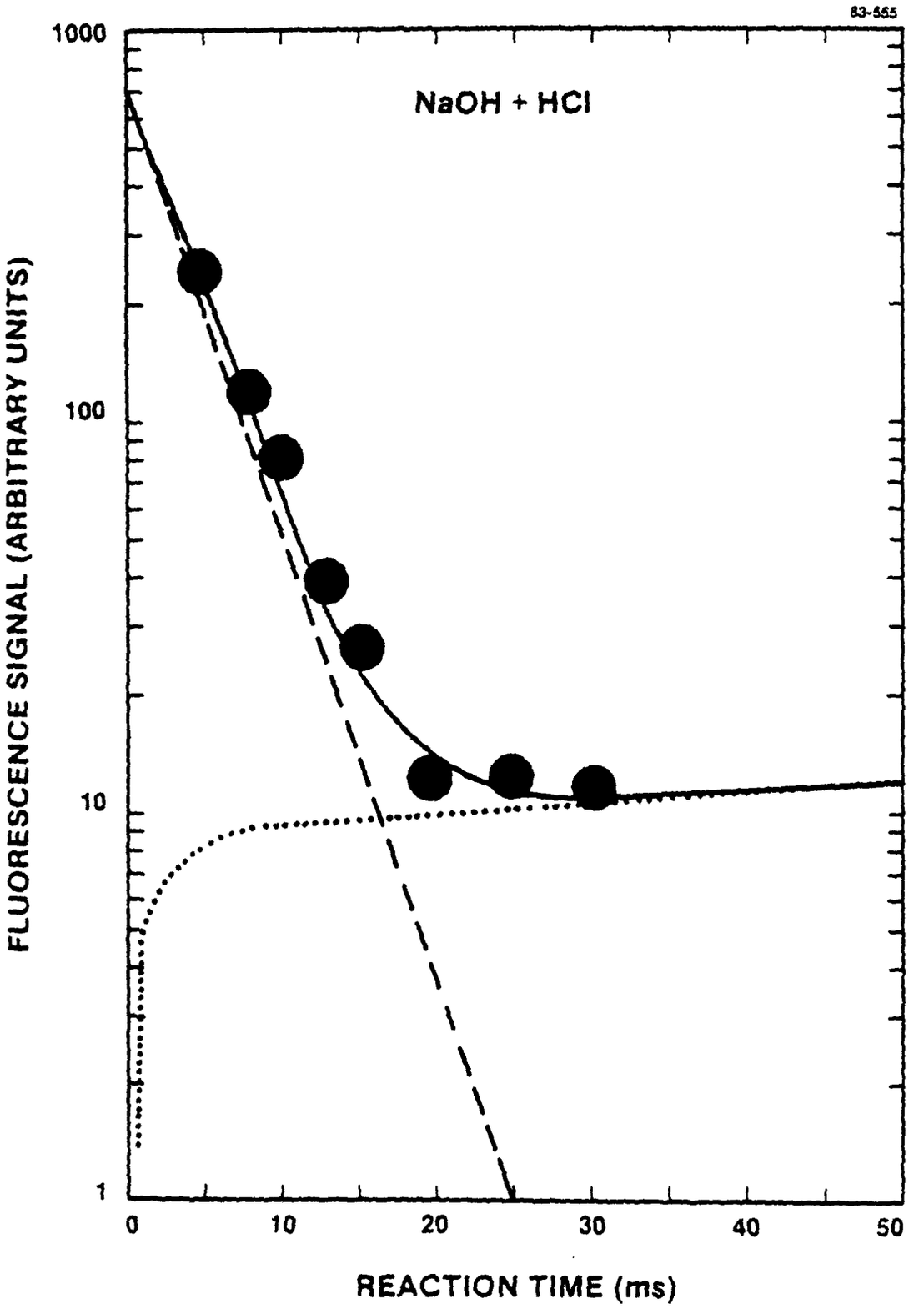

83-565
NaOH + HCl
FLUORESCENCE SIGNAL (ARBITRARY UNITS)
1000
100
10
1
0
10
20
30
40
50
REACTION TIME (ms)

FIGURE 5